UC Irvine
UC Irvine Previously Published Works

Title

Calcium-activated potassium channels in resting and activated human T lymphocytes. Expression levels, calcium dependence, ion selectivity, and pharmacology.

Permalink

https://escholarship.org/uc/item/56k8q6qx

Journal

The Journal of General Physiology, 102(4)

ISSN

0022-1295

Authors

Grissmer, S
Nguyen, AN
Cahalan, MD

Publication Date

1993-10-01

DOI

10.1085/jgp.102.4.601

Copyright Information

Peer reviewed

Calcium-activated Potassium Channels in Resting and Activated Human T Lymphocytes

Expression Levels, Calcium Dependence, Ion Selectivity, and Pharmacology

STEPHAN GRISSMER, ANGELA N. NGUYEN, and MICHAEL D. CAHALAN

From the Department of Physiology and Biophysics, University of California, Irvine, California 92717

ABSTRACT Ca^{2+}-activated $K^+[K(Ca)]$ channels in resting and activated human peripheral blood T lymphocytes were characterized using simultaneous patch-clamp recording and fura-2 monitoring of cytosolic Ca^{2+} concentration, $[Ca^{2+}]_i$. Whole-cell experiments, using EGTA-buffered pipette solutions to raise $[Ca^{2+}]_i$ to 1 μM, revealed a 25-fold increase in the number of conducting K(Ca) channels per cell, from an average of 20 in resting T cells to >500 channels per cell in T cell blasts after mitogenic activation. The opening of K(Ca) channels in both whole-cell and inside-out patch experiments was highly sensitive to $[Ca^{2+}]_i$ (Hill coefficient of 4, with a midpoint of ~300 nM). At optimal $[Ca^{2+}]_i$, the open probability of a K(Ca) channel was 0.3–0.5. K(Ca) channels showed little or no voltage dependence from −100 to 0 mV. Single-channel I-V curves were linear with a unitary conductance of 11 pS in normal Ringer and exhibited modest inward rectification with a unitary conductance of ~35 pS in symmetrical 160 mM K^+. Permeability ratios, relative to K^+, determined from reversal potential measurements were: K^+ (1.0) > Rb^+ (0.96) > NH_4^+ (0.17) > Cs^+ (0.07). Slope conductance ratios were: NH_4^+ (1.2) > K^+ (1.0) > Rb^+ (0.6) > Cs^+ (0.10). Extracellular Cs^+ or Ba^{2+} each induced voltage-dependent block of K(Ca) channels, with block increasing at hyperpolarizing potentials in a manner suggesting a site of block 75% across the membrane field from the outside. K(Ca) channels were blocked by tetraethylammonium (TEA) applied externally (K_d = 40 mM), but were unaffected by 10 mM TEA applied inside by pipette perfusion. K(Ca) channels were blocked by charybdotoxin (CTX) with a half-blocking dose of 3–4 nM, but were resistant to block by noxiustoxin (NTX) at 1–100 nM. Unlike K(Ca) channels in Jurkat T cells, the K(Ca) channels of normal resting or activated T cells were not blocked by apamin. We conclude that while K(Ca) and voltage-gated K^+ channels in the same cells share similarities in ion

permeation, Cs^+ and Ba^{2+} block, and sensitivity to CTX, the underlying proteins differ in structural characteristics that determine channel gating and block by NTX and TEA.

INTRODUCTION

Mitogenic stimulation of human T cells results in an increase in the cytosolic free Ca^{2+} concentration, $[Ca^{2+}]_i$, that is vital for subsequent events leading to cell proliferation and secretion of lymphokines (reviewed by Crabtree, 1989). The initial rise in $[Ca^{2+}]_i$ is caused by the release of Ca^{2+} from intracellular stores by a mechanism involving inositol-1,4,5-triphosphate (IP_3) generation. Ca^{2+} influx is required for the maintained rise in $[Ca^{2+}]_i$, which in some cells consists of $[Ca^{2+}]_i$ oscillations (Tsien, Pozzan, and Rink, 1982; Imboden and Stobo, 1985; June, Ledbetter, Rabinovitch, Martin, Beatty, and Hansen, 1986; Lewis and Cahalan, 1989). In single Jurkat T cells, a leukemic T cell line, investigated with fura-2 ratio imaging, the mitogenic lectin phytohemagglutinin (PHA) induces repetitive $[Ca^{2+}]_i$ oscillations (Lewis and Cahalan, 1989). These oscillations peak at micromolar levels with a period of 90–120 s at room temperature and depend critically upon Ca^{2+} influx from the extracellular medium. Ca^{2+} entry in T cells and Jurkat cells is inhibited by depolarization (Gelfand, Cheung, and Grinstein, 1984; Oettgen, Ter-horst, Cantley, and Rosoff, 1985; Lewis and Cahalan, 1989) and is thought to occur through mitogen-regulated, voltage-independent Ca^{2+} channels (Kuno, Goronzy, Weyand, and Gardner, 1986; Lewis and Cahalan, 1989).

Although Ca^{2+} entry across the plasma membrane would be expected to depolarize the cell, several studies of human T and B cells and mouse thymocytes have shown instead that membrane hyperpolarization accompanies the rise in $[Ca^{2+}]_i$ (Tsien et al., 1982; Felber and Brand, 1983; Wilson and Chused, 1985; Tatham, O'Flynn, and Linch, 1986; MacDougall, Grinstein, and Gelfand, 1988; reviewed by Grinstein and Dixon, 1989). Preliminary fluorescent-indicator studies on individual cells indicate that oscillations in membrane potential accompany the $[Ca^{2+}]_i$ oscillations in Jurkat T cells (Lewis, Grissmer, and Cahalan, 1991). The hyperpolarization can be explained by the presence of K^+ channels that are activated by $[Ca^{2+}]_i$, a conclusion supported by measurements of $^{86}Rb^+$ efflux from cells stimulated with Ca^{2+}-mobilizing agents (reviewed by Rink and Deutsch, 1983; Grinstein and Dixon, 1989). These K^+ channels, by hyperpolarizing the membrane, may facilitate mitogen-regulated Ca^{2+} entry, since a combination of voltage- and calcium-activated K^+ channel blockers has been shown to inhibit mitogen-induced Ca^{2+} oscillations in Jurkat T cells (Grissmer, Lewis, and Cahalan, 1992b).

Recent patch-clamp experiments have provided direct evidence for Ca^{2+}-activated K^+ channels in human B cells and rat thymocytes (Mahaut-Smith and Schlichter, 1989; Partiseti, Choquet, Diu, and Korn, 1992), as well as in Jurkat T cells (Grissmer et al., 1992b). Two types of K(Ca) channels have been described in Jurkat T cells, including a majority of low conductance (5–7 pS) channels that are highly susceptible to block by apamin, a peptide component of bee venom (Grissmer et al., 1992b). In addition, a second, higher conductance channel present at low density and sensitive to the scorpion toxin charybdotoxin (CTX) was described.

In this article, we characterize some biophysical and pharmacological properties of

K(Ca) channels in normal human $CD4^+CD8^-$ and $CD4^-CD8^+$ T lymphocytes before and after activation of the cells with PHA. We have used a combination of whole-cell and excised-patch recording to determine the number of conducting K(Ca) channels per cell and to characterize their $[Ca^{2+}]_i$ dependence, ion selectivity, and sensitivity to a variety of ionic blockers and peptide toxins. Our results indicate that expression of the CTX-sensitive K(Ca) channel increases dramatically after activation. The channel's permeation and pharmacological sensitivity are compared with those of the voltage-gated K^+ channels in the same cells.

Preliminary reports have appeared (Grissmer and Cahalan, 1991; Grissmer, Nguyen, and Cahalan, 1992c; Nguyen, Cahalan, and Grissmer, 1992).

METHODS

Cells

Human peripheral T lymphocytes were isolated from the blood of healthy volunteers. Mononuclear cells were isolated by Ficoll-Hypaque density gradient as described earlier (Cahalan, Chandy, DeCoursey, and Gupta, 1985) and maintained in RPMI 1640 medium supplemented with 1 mM L-glutamine and 10% heat-inactivated fetal bovine serum (Gemini Bioproducts, Calabasas, CA) in a humidified, 5% CO_2 incubator at 37°C. A population of activated T cell blasts was prepared in culture by treating the resting cells with 10 μg/ml PHA (PHA-P; Difco Laboratories Inc., Detroit, MI). In some experiments, cells were incubated with an appropriate dilution of anti-CD4 conjugated with phycoerythrin and anti-CD8 conjugated with fluorescein for 20 min on ice, washed, and resuspended in RPMI 1640 medium containing 10% heat-inactivated fetal bovine serum and 1 mM L-glutamine. The stained cells were plated onto glass chambers and the major T cell subsets were then identified by epifluorescence microscopy. Three populations were evident: orange ($CD4^+CD8^-$ helper T cells), green ($CD4^-CD8^+$ cytotoxic/suppressor T cells), and unstained ($CD4^-CD8^-$ B cells, macrophages, etc.). The glass chambers were coated with poly-L-lysine (0.5 mg/ml) to improve cell adherence to the dish. There was no apparent difference in the numbers and properties of K(Ca) channels found in the helper and cytotoxic suppressor subsets.

Solutions

The cells were bathed in normal Ringer solution containing (mM): 160 NaCl, 4.5 KCl, 2 $CaCl_2$, 1 $MgCl_2$, and 5 HEPES, adjusted to pH 7.4 with NaOH and having an osmolarity of 290–320 mosM. K^+, Rb^+, Cs^+, and Na^+ (0 K^+) Ringer contained 160 mM of the major cation, plus normal Cl^-, divalents, and pH buffering.

K(Ca) channels. For whole-cell recordings, internal (pipette) solutions usually contained (mM): 150 K aspartate, 2 $MgCl_2$, 5 HEPES, 10 EGTA, and 8.7 $CaCl_2$ ($[Ca^{2+}]_{free}$ of 1 μM), adjusted to pH 7.2 with KOH, with an osmolarity of 290–320 mosM. $[Ca^{2+}]_{free}$ was calculated assuming a dissociation constant for EGTA and Ca^{2+} at pH 7.2 of 10^{-7} M (Portzehl, Caldwell, and Ruegg, 1964).

K(V) channels. For whole-cell recordings, internal (pipette) solutions usually contained (mM): 134 KF, 2 $MgCl_2$, 10 HEPES, 1 $CaCl_2$, and 10 EGTA, adjusted to pH 7.2 with KOH, with an osmolarity of 290–320 mosM.

A simple syringe-driven perfusion system was used to exchange solutions in the recording chamber (~250 μl volume) within 15–20 s. A fast solution exchanger for inside-out patch recordings was constructed to deliver solutions from three 1-ml tuberculin syringes (Becton Dickinson and Co., Franklin Lakes, NJ). The tip of each syringe was heated up and pulled to a

final diameter of ~50–100 μm. The ends of the tubing were glued together and placed into the recording chamber. A motorized syringe driver provided continuous flow of solutions. The solution at the cytoplasmic surface of the membrane was changed by positioning the patch into the flow of different syringes. In whole-cell experiments, changing the patch pipette solution was achieved by inserting a tiny quartz pipette (Adams & List Associates, Ltd., Westbury, NY) into the regular patch pipette. The quartz pipette was filled with the solution of choice and was positioned ~1 cm from the tip of the patch pipette. Once the current stabilized in the whole-cell configuration for at least 5 min, the quartz pipette was repositioned ~20 μm from the tip of the patch pipette and slight pressure was applied to the quartz pipette in order to change the patch pipette solution at the tip of the patch pipette.

Ionomycin was purchased from Calbiochem-Novabiochem Corp. (La Jolla, CA), tetraethyl-ammonium chloride (TEA) from Eastman Kodak Co. (Rochester, NY), CTX isolated from scorpion venom from Latoxan (Sepracor, Inc., Marlborough, MA) and recombinant CTX from Peptides International Inc. (Louisville, KY). Noxiustoxin (NTX) was a generous gift from Dr. Robert Slaughter (Merck Institute, Rahway, NJ). BSA (0.1–1 mg/ml; Sigma Chemical Co., St. Louis, MO) was usually added to toxin-containing solutions. Fura-2 was purchased from Molecular Probes, Inc. (Eugene, OR).

Patch-Clamp Recording

Experiments were carried out using standard whole-cell, outside-out, and inside-out recording configurations (Hamill, Marty, Neher, Sakmann, and Sigworth, 1981; Cahalan et al., 1985; Grissmer et al., 1992b). All experiments were done at room temperature (22–26°C). Electrodes were pulled from Accu-fill 90 Micropets (Becton, Dickinson and Co., Parsippany, NJ) in three stages, coated with Sylgard (Dow Corning Corp., Midland, MI), and fire-polished to resistances of 2–7 MΩ. Membrane currents were recorded with a List EPC-7 patch-clamp amplifier (Adams & List Associates, Ltd., Great Neck, NY), usually without series resistance compensation, at a bandwidth of 2 kHz. In several experiments, where the conductance exceeded 5 nS, we used 80% series resistance compensation. Capacitative current was removed by analogue subtraction. The command input of the patch-clamp amplifier was controlled by a PDP 11/73 computer via a digital-to-analog converter (Indec Systems, Inc., Sunnyvale, CA); all command potentials were corrected for the junction potentials of the internal solutions. The holding potential in all experiments was −80 mV. Voltage-ramp stimuli were often used to assess the components of membrane conductance rapidly. Usually the voltage was ramped from −120 to 30 mV within 225 ms every 5 s (sampling rate 457 μs per point) unless otherwise stated. The ramp stimulus results in a small depolarizing shift in the apparent voltage dependence for the voltage-gated K^+ channels, relative to that determined by voltage steps. Because the K(Ca) channels are voltage independent, slope conductances at potentials more negative than −20 mV are proportional to the number of open K(Ca) channels.

Measurement of $[Ca^{2+}]_i$

In experiments combining patch-recording with fura-2 measurement, a photomultiplier tube (model 647-04; Hamamatsu Photonic Systems Corp., Bridgewater, NJ) and photon-counting photometer (model 126; Pacific Instruments, Inc., Concord, CA) were used to collect light under program control from a patch-clamped cell. Light from a Newport 75-W xenon arc lamp was diverted by a beam splitter through two shuttered light paths containing 10-nm band-pass filters centered at either 350 or 385 nm. Alternating the shutters while limiting the light exposure to 200 ms per 1.2 s data collection cycle provided fura-2 light excitation and minimized photobleaching. The photometer output was sampled and processed on-line using the patch-clamp interface, as described elsewhere (Lewis and Cahalan, 1989). Cell calibrations

of $[Ca^{2+}]_i$ with a K_d of 225 nM for fura-2 inside the cell were used in simultaneous patch and fura-2 experiments (cf. Almers and Neher, 1985; Negulescu and Machen, 1991).

RESULTS

Patch-clamp studies have shown that resting T lymphocytes separated from human peripheral blood (HPB) have an average of 400 voltage-gated K⁺ [K(V)] channels per cell (Cahalan et al., 1985). A second population of K⁺ channels in normal T cells can be opened if $[Ca^{2+}]_i$ is elevated above 100 nM either by whole-cell dialysis from a highly buffered Ca-EGTA pipette solution or by treating a lightly buffered cell with PHA or ionomycin. As described below, these K(Ca) channels were readily distin-
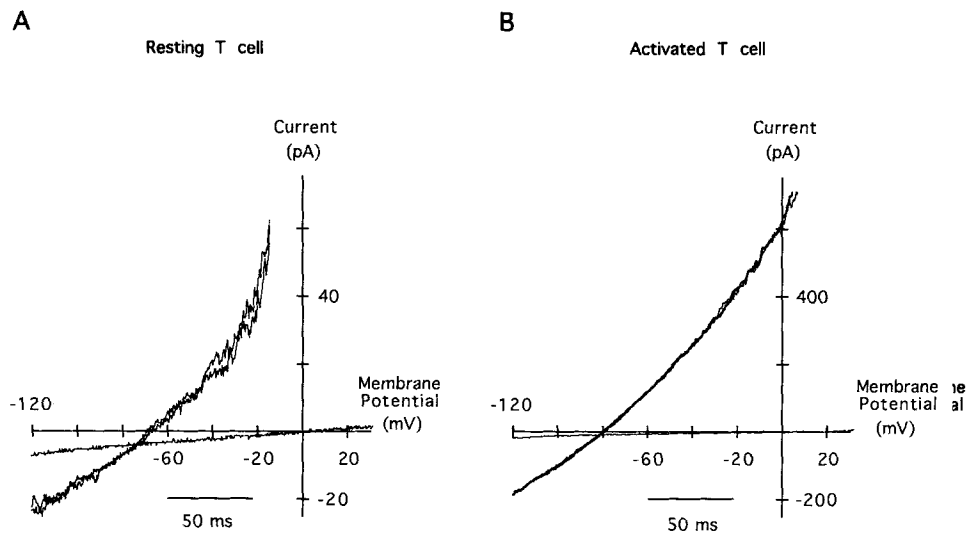
A
Resting T cell

B
Activated T cell

FIGURE 1. Expression of K(Ca) channels in resting (*A*) and activated (*B*) HPB T lymphocytes. K(Ca) channels were opened by whole-cell dialysis with pipette solutions containing 1 μM free $[Ca^{2+}]$. Ramp currents were elicited by 225-ms voltage ramps from −120 to 30 mV delivered every 5 s before and after establishing the whole-cell recording mode. The cell in *B* was activated by the mitogenic lectin, PHA (10 μg/ml), for 4 d.

guished by their single-channel conductance and pharmacological profile from a population of apamin-sensitive K(Ca) channels in a leukemic T cell line, Jurkat (Grissmer et al., 1992b).

Activation of K(Ca) Channels during Whole-Cell Recording

A voltage-ramp protocol enabling rapid measurement of conductances was used to reveal the presence of K(Ca) channels during whole-cell dialysis with a pipette solution containing 1 μM free $[Ca^{2+}]_i$ (Fig. 1). The flat trace, recorded in the cell-attached recording mode before break-in, reflects the seal resistance (~20 GΩ). The patch was then ruptured with suction to initiate whole-cell recording, yielding a ramp current after dialysis with a slope conductance of 0.5 nS. The ramp current

after break-in reverses near −80 mV, suggesting the induction of a K^+-selective conductance. K^+ selectivity was confirmed by external solution exchange, as discussed in detail below. In 18 experiments of this type, the slope conductance for the K(Ca) channels near −80 mV was determined to be 0.2 ± 0.1 nS (mean ± SEM; n = 18) in resting T cells bathed in normal Ringer. Current through voltage-gated K^+ channels can also be observed in many of the records as an upward deflection at more positive potentials. The ramp protocol with elevated $[Ca^{2+}]_i$ reduces the size of voltage-gated currents, because the use-dependent inactivation exhibited by K(V) channels during repetitive depolarization is accentuated by calcium ions from the inside (Cahalan et al., 1985; Bregestovski, Redkozubov, and Alexeev, 1986; Grissmer and Cahalan, 1989b).

Increased Channel Numbers in T Cell Blasts

Using similar procedures, we found that activated T cell blasts express many more K(Ca) channels than resting HPB T lymphocytes; on average, ramp currents elicited by dialysis with elevated $[Ca^{2+}]_i$ were 30-fold larger (Fig. 1 B). In cells activated for more than 2 d, the K(Ca) conductance, $g_{K(Ca)}$, was 6.4 ± 0.5 nS in normal Ringer solution (mean ± SEM, n = 69). Assuming a single-channel conductance of 11 pS in Ringer (see below), the number of conducting channels increases from ∼20 per resting cell to ∼500 after the cell becomes activated and enters the cell cycle. Activated T cells are enlarged relative to resting cells. The whole-cell capacitance of cells selected for patch-clamping in our experiments increased from 2 ± 0.2 pF (mean ± SEM, n = 18) to 5 ± 0.2 pF (mean ± SEM, n = 69). Thus, the increased number of K(Ca) channels reflects an increase primarily in the surface density of channels. For further characterization of the K(Ca) channels we routinely used activated T cells.

The increased numbers of K(Ca) channels occurred in both helper and cytotoxic/suppressor phenotypes, identified by the cell-surface antigens CD4 and CD8, respectively. Fig. 2 illustrates the increased K(Ca) channel numbers at various times after activation by PHA of T cells in culture. Both $CD4^+CD8^-$ (helper) and $CD4^-CD8^+$ (suppressor/cytotoxic) HPB T lymphocytes show increased numbers of channels after several days of activation with PHA.

In parallel whole-cell experiments using a KF pipette solution, we compared the K(V) conductance, $g_{K(V)}$, through voltage-gated K^+ channels in resting and activated T cells. The KF pipette solution buffered $[Ca^{2+}]_i$ to <10 nM, thereby preventing the opening of K(Ca) channels. In response to step depolarization, K(V) channels open and slowly inactivate. From the peak current measured at +40 mV, within the plateau region of the g_K-V relation, the conductance increased from 4.9 ± 1.3 nS in 15 resting cells to 16.6 ± 10.4 nS in 21 chronically activated (3–6 d) T cell blasts. The increase in $g_{K(V)}$ parallels the increased membrane surface area of the activated T cells. The specific $g_{K(V)}$ values normalized by the measured membrane capacitance did not change significantly (2.2 ± 0.8 nS/pF in resting cells vs. 2.5 ± 1.9 nS/pF in activated cells). Thus, both $g_{K(V)}$ and $g_{K(Ca)}$ increase as T cells enlarge and begin to proliferate in response to PHA, but the surface density of K(Ca) channels is specifically increased during activation.
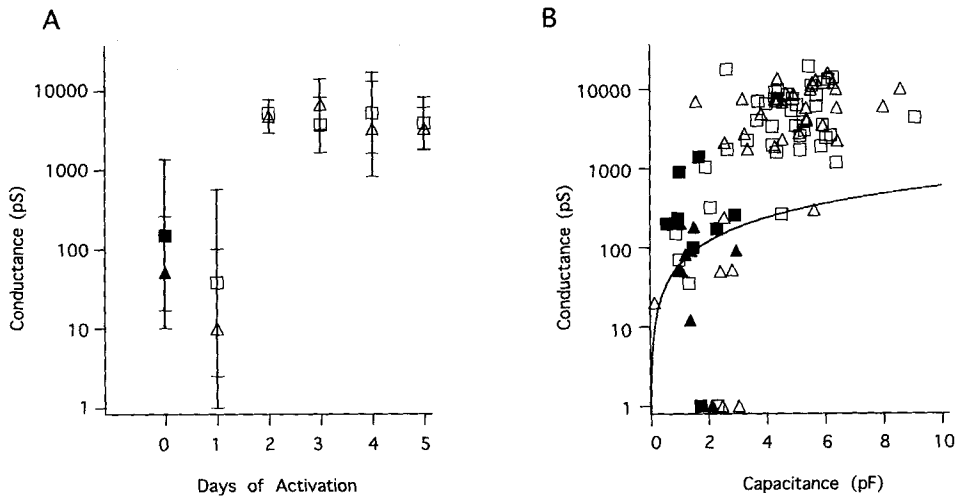
A

B

FIGURE 2. Increase in K(Ca) channel expression in CD4⁺CD8⁻ (*squares*) and CD4⁻CD8⁺ (*triangles*) HPB T lymphocytes after activation with 10 μg/ml PHA. Resting (unactivated) T cells are indicated by filled symbols. (*A*) Conductance of whole-cell K(Ca) current, $g_{K(Ca)}$, as a function of days of activation by PHA. Each data point represents the geometric mean ± SD of $g_{K(Ca)}$ for at least six cells in each T cell subset. (*B*) Capacitance of each cell, as an indicator of cell size, plotted versus $g_{K(Ca)}$ in the same cell. The curve indicates scaling relative to the mean $g_{K(Ca)}$ of resting T cells. Most of the activated cells (*open symbols*) lie above this curve, indicating increased K(Ca) channel density.

Time Course of K(Ca) Channel Activation during Dialysis

K(Ca) channels opened rapidly and remained stable when $[Ca^{2+}]_i$ was elevated by whole-cell dialysis. Fig. 3 *A* illustrates currents before and after break-in to achieve whole-cell recording with a pipette solution containing 1 μM $[Ca^{2+}]_i$. The first trace after break-in is flat at potentials between −100 and −60 mV, indicating a low internal calcium concentration at the time of break-in. At depolarized potentials, K(V) channels were opened during the ramp, giving rise to an increase in slope conductance above −20 mV. As dialysis proceeded, successive ramp currents with increasing slope appeared to pivot around −80 mV, indicating the activation of K(Ca) channels. The time course for the induction of the K(Ca) channels is illustrated in Fig. 3 *B*. The transition from cell-attached to whole-cell recording ($t = 0$ s) marks the time at which the Ca²⁺-EGTA mixture in the pipette started to diffuse into the cell. Within 2 s, the activation of the conductance was already complete, reaching a plateau value of ∼5 nS. Fig. 3 *C* shows slope conductance values in another experiment on a prolonged time scale, demonstrating that currents through K(Ca) channels remained stable during whole-cell recording over a period of at least 10 min.

K(Ca) Channels Are Voltage Independent

The K⁺ current activated by elevated $[Ca^{2+}]_i$ did not exhibit kinetic relaxations during voltage steps. In recordings made with low Ca²⁺ in the pipette (Fig. 4 *A*), the

current was carried primarily by the K(V) channels, along with a small leakage conductance. In a cell with elevated $[Ca^{2+}]_i$ (Fig. 4 B), the voltage- and time-dependent currents are superimposed on steps of current with a reversal potential indicating K^+ permeability. These data suggest that raising $[Ca^{2+}]_i$ activates a voltage-independent K^+ current.
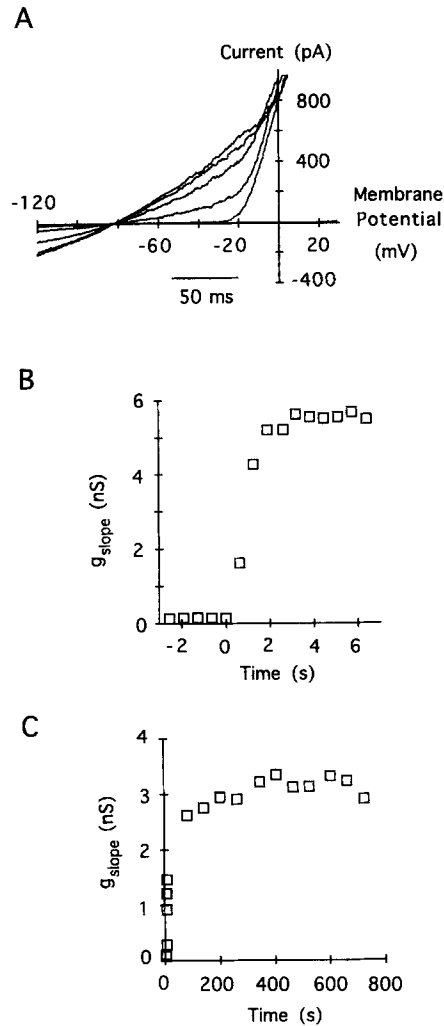

FIGURE 3. Opening and stability of K(Ca) channels in PHA-activated HPB T lymphocytes during whole-cell dialysis with 1 μM free Ca^{2+}. (A) Ramp currents before and after break-in. Currents were recorded during voltage ramps delivered every 625 ms before and after establishing the whole-cell recording mode. Ramp currents recorded immediately before the transition from the cell-attached to the whole-cell recording mode are represented by the flat trace. The subsequent traces show an increase in slope conductance at potentials between −100 and −60 mV, with a crossover of the ramp currents at approximately −80 mV, suggesting induction of a K^+-selective conductance. (B) Time course of K(Ca) channel activation. K(Ca) conductance, $g_{K(Ca)}$, was determined for each ramp current by fitting a line to the data points between −100 and −60 mV. These conductance values are plotted as a function of time before and after break-in for the experiment shown in A. Access resistance was 16 MΩ during this experiment. (C) Stability of $g_{K(Ca)}$. Conductance values determined as described above plotted on a longer time base for another cell. Access resistance was 14 MΩ throughout this experiment.

Dependence on $[Ca^{2+}]_i$ in Whole-Cell Measurements

Simultaneous whole-cell and fura-2 measurements enabled a direct comparison of $g_{K(Ca)}$ and $[Ca^{2+}]_i$. In the experiment illustrated by Fig. 5, $[Ca^{2+}]_i$ increased right after the transition from the cell-attached to the whole-cell recording mode, decreased after application of a Ca^{2+}-free Ringer solution, and increased rapidly after applica-

tion of a Ca²⁺-containing Ringer solution with 1 μM ionomycin. K(Ca) current was activated with an overlapping time course. The change in slope conductance shown in Fig. 5 B, determined from the ramp records in Fig. 5 A, suggests that the conductance is activated as $[Ca^{2+}]_i$ rises, and then saturates as $[Ca^{2+}]_i$ nears 1 μM. Similar results were found in nine other cells. However, in the majority of the cells, a shift of the reversal potential toward more positive potentials could be observed when $[Ca^{2+}]_i$ reached levels >1 μM, indicating the induction of a leak conductance in addition to the K(Ca) conductance.

Fig. 5 C illustrates the calcium dependence of the K(Ca) channels in an activated HPB T lymphocyte. Plotting, point by point in time, the slope conductance, determined from ramp currents, as a function of the $[Ca^{2+}]_i$ estimated from fura-2 fluorescence ratios, yields the calcium dependence of the conductance. A curve describing the cooperative binding of a ligand with an exponent of 4 (Hill, 1910) fits the data. This approach suggests that K(Ca) channels are steeply dependent upon

A

$[Ca^{2+}]_i$ = 10 nM

B

$[Ca^{2+}]_i$ = 1 μM

400 pA |___
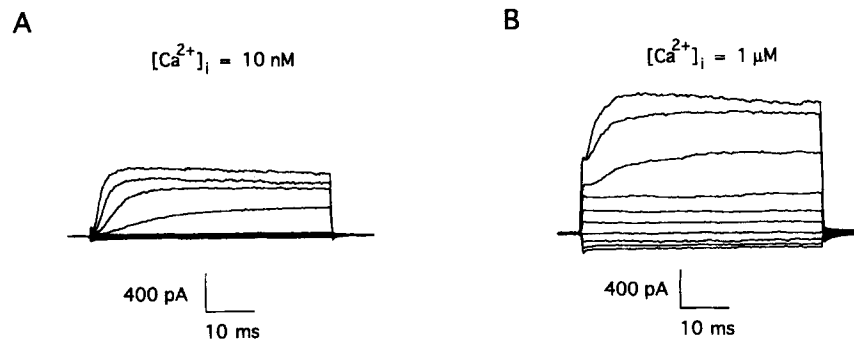   10 ms

400 pA |___
        10 ms

FIGURE 4. $I_{K(V)}$ and $I_{K(Ca)}$ in PHA-activated HPB T lymphocytes. Currents were elicited with 50-ms hyper- and depolarizing voltage steps from a holding potential of −80 to −140 to +40 mV in 20-mV increments every 30 s. (A) Only voltage-gated K⁺ channels can be elicited when using pipette solutions buffering $[Ca^{2+}]_i$ to 10 nM. (B) Voltage-gated and Ca²⁺-activated K⁺ channels can be elicited using pipette solutions containing 1 μM Ca²⁺.

$[Ca^{2+}]_i$, with activation beginning above 200 nM and saturating at ~1 μM. The result indicates that binding of four or more Ca²⁺ ions may be required to open the channel. Similar results were obtained in nine experiments, yielding an estimated K_d value of 310 ± 86 nM (mean ± SD) with a Hill coefficient of 3.9 ± 0.6.

K(Ca) Channels in Inside-Out Patches: Calcium Dependence

In activated T cell blasts, K(Ca) channel density is high enough that most excised patches, either outside-out or inside-out, contain at least one K(Ca) channel. Fig. 6 illustrates an inside-out patch that appeared to contain just one channel that responded to altered [Ca²⁺] applied to the cytoplasmic membrane surface. With no added Ca²⁺ and 10 mM EGTA, the channel was always silent. Raising [Ca²⁺] to 0.3 and 1 μM resulted in increased channel activity, which then declined upon exposure to 10 μM [Ca²⁺]. Amplitude histograms, shown in Fig. 6 B below the corresponding examples of current records in Fig. 6 A, demonstrate the changes in open probabili-
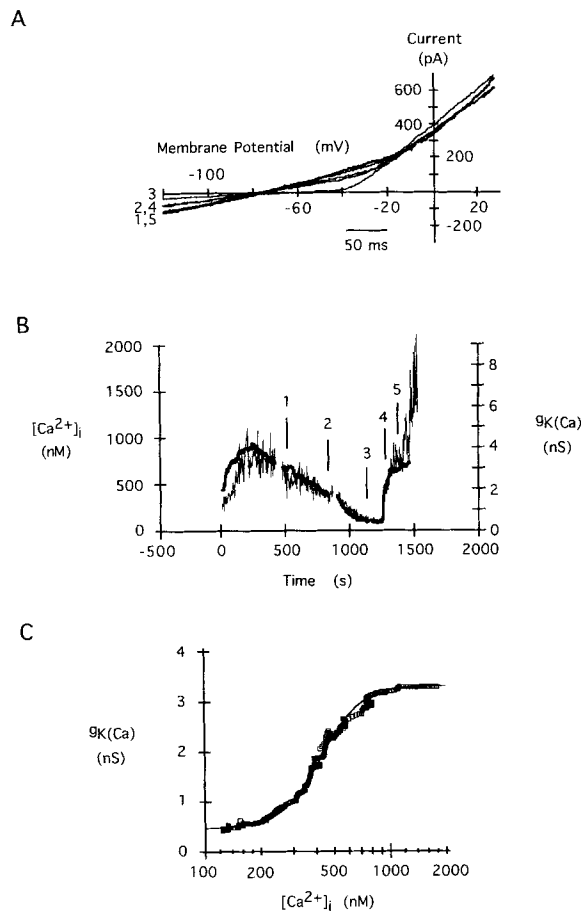
A

B

C

FIGURE 5. Simultaneous measurement of whole-cell ramp currents and $[Ca^{2+}]_i$ after the transition from the cell-attached to the whole-cell recording mode and during application of 1 μM ionomycin in HPB T lymphocytes. (*A*) Ramp currents were elicited every second. Traces *1–5* were taken at different times during the experiment. (*B*) Superimposed time course of the change in $[Ca^{2+}]_i$ and the activation of the Ca^{2+}-activated K^+ channels. The slope conductance of the ramp currents obtained as described in the legend to Fig. 3 *A* was used as a measure of activation of the Ca^{2+}-activated K^+ channels and plotted (*dark trace*) against the appropriate times during the experiment. Simultaneously, $[Ca^{2+}]_i$ measurements were obtained and are plotted (*light trace*) for comparison. The numbers on the graph correspond to the ramp currents shown in *A*. The pipette solution contained 160 mM K aspartate, 5 mM HEPES, 2.0 mM MgCl₂, 0.3 mM EGTA, and 100 μM fura-2. The cell was initially bathed in normal Ringer solution; $[Ca^{2+}]_i$ spontaneously increased after the transition to whole-cell recording. To lower $[Ca^{2+}]_i$, we applied a Ringer solution with no added Ca^{2+} 200 s after the start of the experiment. At 1,300 s we applied 1 μM ionomycin in normal Ca^{2+}-containing Ringer. (*C*) Ca^{2+} sensitivity of K(Ca) channels in activated HPB T lymphocytes. The slope conductance value for each time point is plotted against the corresponding $[Ca^{2+}]_i$ determined from the fura-2 ratio. The resulting curve includes both the rising and falling phases of the ionomycin-induced $[Ca^{2+}]_i$ transient illustrated in *B*. The data points are fitted by eye using the following equation:

$$g_{K(Ca)} = g_1 + g_{K(Ca)max}/[1 + (K_d/[Ca^{2+}]_i)^x]$$

with an offset representing the background slope conductance (g_1) of 0.46 nS, a maximum slope conductance ($g_{K(Ca)max}$) of 2.85 nS, $K_d = 425$ nM, and $x = 4$.

ties. From these histograms, the channel appears to be highly sensitive to $[Ca^{2+}]_i$ within the 100 nM–1 μM range, and has a single-channel current of 3 pA at −80 mV.

We calculated and averaged the open probability, P_o, of single K(Ca) channels as a function of $[Ca^{2+}]$ exposed to the cytoplasmic membrane. At the optimal $[Ca^{2+}]$ of 1

μM, K(Ca) channels are not open all the time; the maximum P_0 of single K(Ca) channels is ~ 0.4. The smooth curve in Fig. 6 C represents the average Ca^{2+} sensitivity from whole-cell/fura-2 measurements. The change in whole-cell conductance in response to varying $[Ca^{2+}]_i$ can be accounted for by a change in the P_0 of the single channels.

An analysis of open and closed durations of single K(Ca) channels is illustrated in Fig. 7. At a cytosolic $[Ca^{2+}]$ of 1 μM, the distribution of open times could be reasonably well fitted by a single exponential function with a mean open time averaging 8.3 ± 2.4 ms (mean $\pm$ SD, $n = 12$ patches). A sum of two exponentials provided a reasonable fit to the closed intervals, indicating closed times of 1.7 ± 1.0 ms ($73 \pm 8\%$) and 15.4 ± 6.9 ms ($27 \pm 8\%$, $n = 12$ patches). We have not pursued a detailed kinetic description of the $[Ca^{2+}]_i$ and voltage dependence of these single-channel lifetimes.

Single-Channel Current–Voltage Relations: Conductance and Uniformity of K(Ca) Channels

We determined the single-channel current–voltage relation of the K(Ca) channels in outside-out patches from activated HPB T lymphocytes. Fig. 8 A illustrates a patch containing two K(Ca) channels, each with a single-channel conductance of ~ 11 pS. Openings could be observed over the entire voltage-ramp range, suggesting little if any voltage-dependent gating. In another patch, with K^+ Ringer as the bath solution (Fig. 8 B), we were able to measure the opening of a single channel with a conductance of 35 pS at hyperpolarized potentials and 11 pS at depolarized potentials.

In Jurkat T cells, the majority of K(Ca) channels exhibited lower single-channel conductance values (5 pS in K^+ Ringer; Grissmer et al., 1992b) compared with those described in Fig. 8 for normal human T cells. Is the current seen in whole-cell recordings from normal human T cells due to the activation of a single population of K(Ca) channels, or to a mixture of different K(Ca) channel populations that can be distinguished on the basis of their single-channel amplitudes? In normal T cell blasts, the 35-pS channel was by far the most commonly observed K(Ca) channel. An example of an inside-out patch displaying the activity of five K(Ca) channels is shown in Fig. 9 A. The corresponding amplitude histogram (Fig. 9 B) demonstrates that the peaks, corresponding to the opening of different numbers of channels, are uniformly ~ 3 pA apart from each other, indicating only one single-channel conductance of ~ 35 pS for all five channels. We cannot, however, exclude the existence of one or more minor populations of K(Ca) channels.

Ion Selectivity of K(Ca) Channels

The single-channel conductance (11 pS in Ringer, 35 pS in K^+ Ringer) and I-V shape of K(Ca) channels is similar to that for K(V) channels in T lymphocytes reported previously (Cahalan et al., 1985). We therefore compared the ion selectivity and sensitivity to blockers for both channel types. To open the K(Ca) channels, we used whole-cell dialysis with 1 μM free $[Ca^{2+}]$ and varied the external cationic species while measuring the change in slope conductance and reversal potential during voltage ramps, as shown in Fig. 10 A. Increasing external K^+ from 4.5 to 160 mM
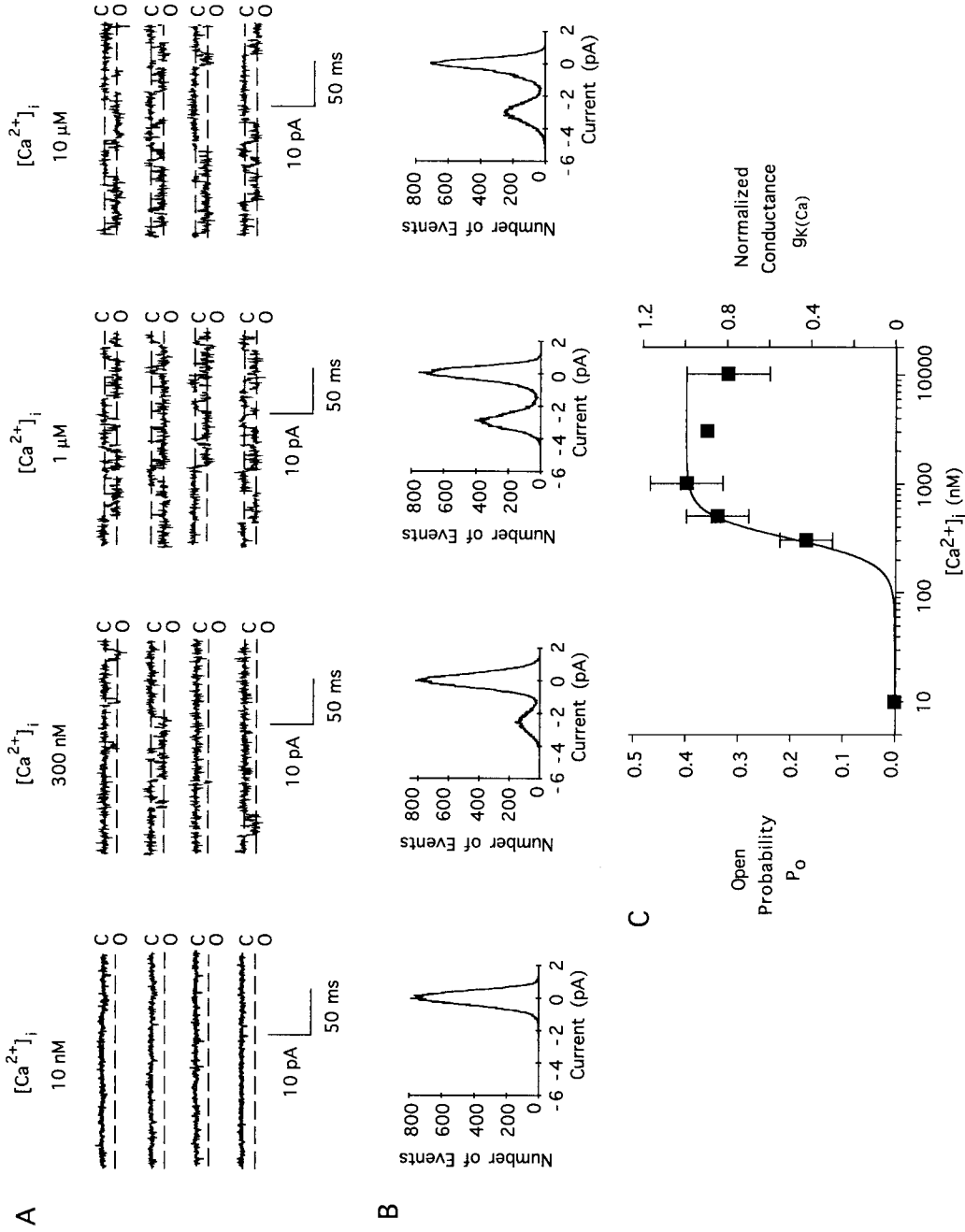
FIGURE 6

$[Ca^{2+}]_i = 1 \mu M$

A

120

Number of Events

80

40

0

Open times

$\tau_O = 9$ ms

0   20   40   60   80   100

Time (ms)

B

500

400

Number of Events

300

200

100

0

Closed times

$\tau_{C1} = 2.5$ ms

$\tau_{C2} = 20$ ms

0   20   40   60   80   100

Time (ms)
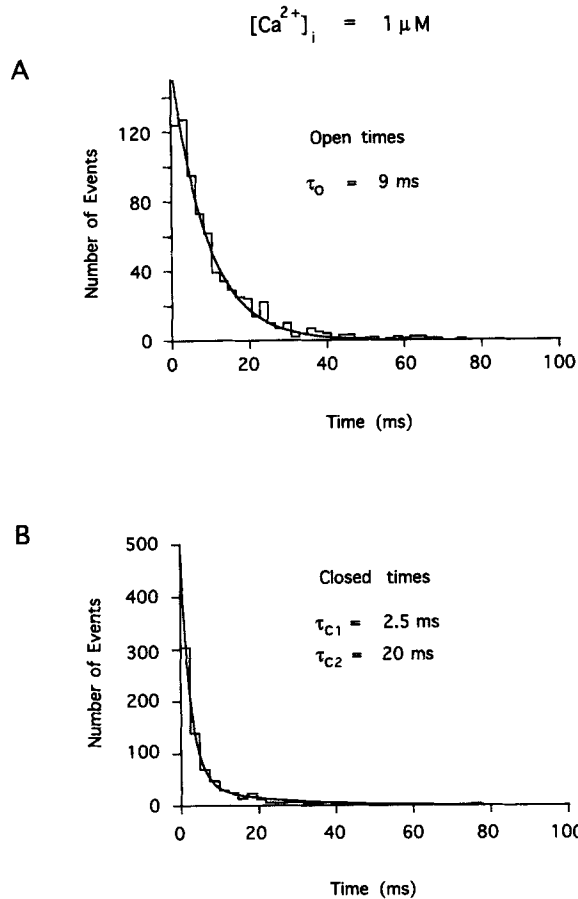
FIGURE 7. Open- and closed-time distributions in an inside-out patch from an activated HPB T lymphocyte. The pipette solution was K⁺ Ringer. Current was continuously recorded on tape with a bandwidth of 5 kHz at a holding potential of −80 mV with K aspartate buffered to 1 μM Ca²⁺ as bath solution. A total of 2,252 events was analyzed in this patch. (*A*) Open-time distribution showing a single exponential fit with a mean open time of 9.0 ms. (*B*) Closed-time distribution showing a double exponential function, yielding mean closed times of 2.5 and 20.0 ms, with relative amplitude coefficients A1 and A2 of 90 and 10%, respectively.

FIGURE 6 (*opposite*). Ca²⁺ sensitivity of a single K(Ca) channel in the inside-out configuration from an activated HPB T lymphocyte. The pipette solution was K⁺ Ringer. Solutions containing varying [Ca²⁺] were applied to the cytoplasmic membrane surface from tubes (∼100 μm in diameter). Examples of original current traces recorded at a holding potential of −80 mV with K aspartate buffered to the indicated Ca²⁺ concentrations as bath solution (*A*), along with corresponding amplitude histograms (*B*). The peak on the right represents the current when the channel is closed, while the peak on the left is the open-channel level. The single-channel amplitude, measured as the difference between the two amplitude peaks, is ∼3 pA. (*C*) P_o of a single K(Ca) channel as a function of the Ca²⁺ concentration facing the cytoplasmic site of the channel. The P_o reflects the fractional time the channel spends in the open state compared with the total recording time. P_o was calculated for each [Ca²⁺] by fitting Gaussian distributions to the amplitude histograms, examples of which are shown in *B*; the fractional area under the open distribution corresponds to P_o. The smooth line in the graph was drawn according to the equation shown in the legend of Fig. 5, with the average value for K_d of 310 ± 86 nM (mean ± SD, n = 9) and a Hill coefficient of 3.9 ± 0.6 (mean ± SD, n = 9).

increased the slope conductance from 10 to 36 nS at potentials more negative than −60 mV. Voltage-gated K^+ channels can be seen to activate at potentials more positive than −40 mV, giving rise to an increase in inward current around −20 mV. To determine the reversal potential, E_R, for current flow through K(Ca) channels, we selectively blocked K(V) channels with a peptide scorpion toxin, NTX, in this series of experiments (for details on the NTX block, see Fig. 15 below). E_R changed from −80 mV in Na^+ Ringer to −40, 3, and 4 mV in NH_4^+, Rb^+, and K^+ Ringer, respectively. From these changes in E_R, the calculated permeability ratios, P_X/P_K, for the K(Ca)
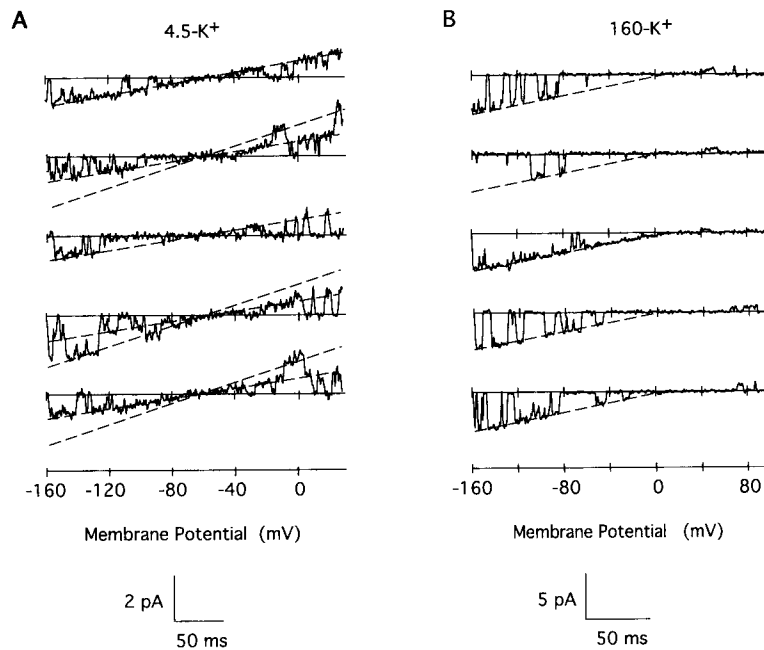

FIGURE 8. Single-channel recordings of K(Ca) channels in two outside-out patches from activated HPB T lymphocytes. K(Ca) channels were activated by whole-cell dialysis with pipette solutions containing 1 μM free $[Ca^{2+}]$. After the transition from the whole-cell to the outside-out configuration, ramp currents were elicited by 450-ms voltage ramps from −160 to 30 mV in A and from −160 to 100 mV in B every 5 s (holding potential −80 mV). Bath solutions were normal mammalian Ringer (A) and K^+ Ringer (B), respectively. The dotted lines through the current records were drawn for clarity and represent slope conductances of 11 and 22 pS in A and 35 pS in B.

channel are 1.0, 0.96, and 0.17 for K^+, Rb^+, and NH_4^+, respectively. These permeability ratios are slightly different from those obtained for the voltage-gated K^+ channel by measuring instantaneous tail currents after a short conditioning prepulse to +40 mV. From the instantaneous I-V relations seen in Fig. 10 B, we measured E_R and calculated P_X/P_K for K(V) to be 1.0, 0.82, and 0.13 for K^+, Rb^+, and NH_4^+, respectively.

A similar approach was used to test for Na^+ and Cs^+ permeability through K(Ca) channels. With K^+-free Na^+ Ringer, no inward current through K(Ca) channels was

observed, and 20 nM CTX blocked most of the outward current (Fig. 10 C). The I-V relationships in the presence and absence of CTX converge near -140 mV. Taking this as a limit, the permeability ratio, P_{Na}/P_K, would be <0.004. With Cs^+ Ringer, inward currents were observed below a reversal potential of -66 ± 5 mV ($n = 5$ cells), suggesting a permeability ratio, P_{Cs}/P_K, of 0.073 (Fig. 10 D). Surprisingly, these currents were not blocked by 20 nM CTX. Two interpretations for the lack of
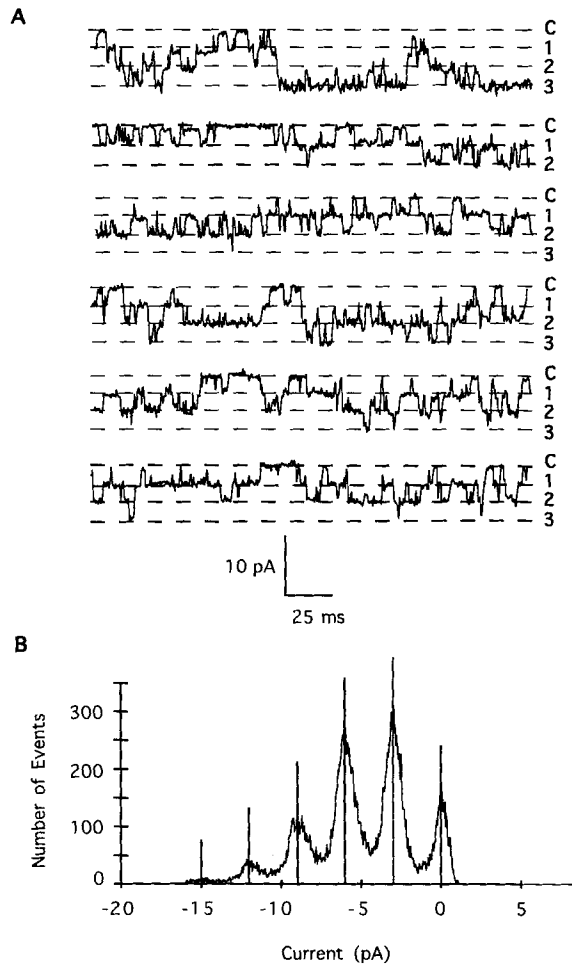
A

B

FIGURE 9. Activation of five K(Ca) channels by 1 µM Ca^{2+} in an inside-out patch from an activated HPB T lymphocyte. (A) Examples of original current traces recorded at a holding potential of -80 mV with K-aspartate buffered to 1 µM Ca^{2+} as bath solution. The pipette solution was K^+ Ringer. (B) Amplitude histogram. The peak on the very right represents the current when all five channels are closed, while the peaks on the left represent the current when different numbers of channels are open. The single-channel amplitude, measured as the difference between peaks, is ~ 3 pA.

CTX block in Cs^+-containing solution are possible: Cs^+ may compete with CTX for its binding site on the K(Ca) channel, or current through a different channel may be reversibly induced in Cs^+ solution. We favor the former interpretation, because: (a) in control experiments with a low $[Ca^{2+}]_i$ pipette solution, there was no change in the I-V below -60 mV (i.e., the Cs^+ current is $[Ca^{2+}]_i$ dependent); and (b) replacing most of the Cl^- in the bathing solution with aspartate did not alter the reversal potential

(i.e., the current is not a Cl⁻ current). We titrated the Cs^+ effect on CTX block by varying the percentage of Cs^+ in the bath and found that 40 mM Cs^+ inhibited the block by 20 nM CTX by ~50% (not shown). Cs^+ ions, in addition to being sparingly permeant, block K^+ current through K(Ca) channels in a voltage-dependent manner, as described below.
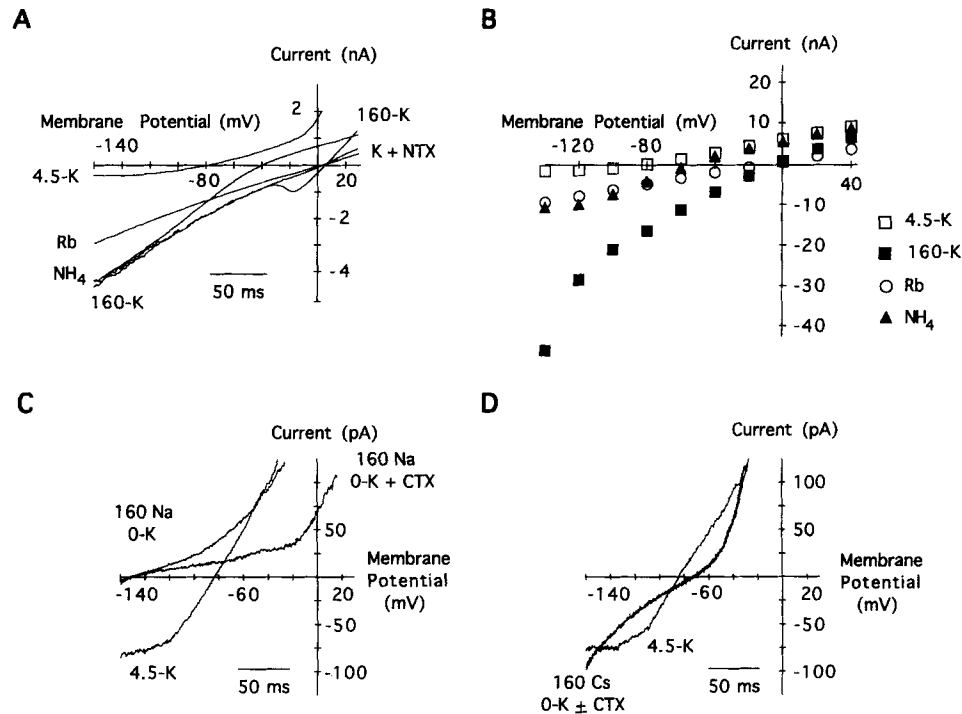

FIGURE 10. Selectivity sequence of monovalent cations in K(V) and K(Ca) channels in HPB T lymphocytes. (A) K(Ca) channels were activated during whole-cell dialysis with pipette solutions containing 1 μM free Ca^{2+}. Ramp currents were elicited by 225-ms voltage ramps from −160 to 30 mV every 5 s before and during the application of K^+ Ringer, NH_4^+ Ringer, and Rb^+ Ringer. (B) Instantaneous I-V relationship for K(V) channels in normal Ringer (160 mM Na^+ with 4.5 mM K^+ [□]), 160 mM K^+ Ringer (■), 160 mM Rb^+ Ringer (○), and 160 mM NH_4^+ Ringer (▲). Instantaneous currents were measured during test pulses after 15-ms prepulses to +40 mV in order to maximally activate the K(V) conductance. The series resistances in both types of experiments were between 5 and 10 MΩ. (C) K(Ca) channels were activated as in A. Removal of K^+ from normal Ringer eliminated inward current through K(Ca) channels; most of the remaining outward current was blocked by 20 nM CTX. (D) K(Ca) channels were activated as in A and C. The bath solution was changed from normal Ringer to 160 mM Cs^+ Ringer lacking K^+. Subsequent addition of 20 nM CTX did not alter the I-V relation, as indicated.

In addition to permeability ratios, we determined the conductance ratios of K(V) and K(Ca) channels by measuring the slope of the instantaneous tail current I-V curve for K(V) channels (Fig. 10 B), or the slope of the ramp current between −100 and −60 mV for K(Ca) channels (Fig. 10 A, Table I). Both the permeability and the conductance ratios suggest that K(Ca) channels are less selective than K(V) channels.

The most striking difference between the two channels is the ability to carry NH_4^+ inward current; relative to K^+, NH_4^+ carries current more effectively through K(Ca) channels than through K(V) channels.

Pharmacology of K(Ca) Channels

Metal cations. Channel blockers provide a further basis of comparison between the K(Ca) and K(V) channels. In the presence of 16 mM external Cs^+, both channel types become increasingly blocked at hyperpolarized potentials. We determined the steepness of the Cs^+ block of K(Ca) channels by measuring ramp currents in K^+ Ringer solution and K^+ Ringer with 16 mM Cs^+ (Fig. 11 *A*). This procedure provides an accurate steady-state measure, because Cs^+ block is very rapid compared with the rate of the voltage-ramp stimulus. We formed ratios of the ramp currents in the presence and absence of Cs^+ (Fig. 11 *B*) and fitted the ratios with a Boltzmann relation, as described in the legend of Fig. 11. Cs^+ block of K(Ca) channels in HPB T lymphocytes is as steep as expected from the movement of a single monovalent cation about three-quarters into the electric field of the membrane ($\delta = 0.78 \pm 0.04$,

TABLE I

Permeability and Conductance Ratios of K(V) and K(Ca) Channels in Human T Lymphocytes

	P_X/P_K				g_X/g_K			
	K^+	Rb^+	NH_4^+	Cs^+	K^+	Rb^+	NH_4^+	Cs^+
K(Ca)	1.0	0.96	0.17	0.07	1.0	0.7	1.2	0.1
K(V)	1.0	0.82	0.13	ND	1.0	0.40	0.67	ND
K(V)*	1.0	0.77	0.1	0.02	1.0	0.5	0.25	ND

ND, not determined.
*Data from Cahalan et al., 1985. In that study, g_X/g_K values were determined from the chord conductance measured at 0 mV.

where δ represents the equivalent electrical distance from the external surface of the membrane; mean $\pm$ SD, $n = 3$). The steepness factor, k, in the Boltzmann equation was 32 ± 2 mV (mean $\pm$ SD; $n = 3$). Similar values were obtained for the Cs^+ block of K(V) channels, as shown in Fig. 11, *C* and *D*. Thus the sites of Cs^+ block are likely to be similar in both K(Ca) and K(V) channels.

In similar experiments, we investigated Ba^{2+} block of K(Ca) channels (Fig. 12). Ba^{2+} block from the external solution was voltage dependent and as steep as expected from the movement of a single divalent cation about three-quarters into the membrane field ($\delta = 0.74 \pm 0.04$; mean $\pm$ SD, $n = 3$). The steepness factor, k, was 17 ± 1 mV (mean $\pm$ SD; $n = 3$). We conclude that Cs^+ and Ba^{2+} bind at a site or sites similar in their electrical distance across the membrane. Block of K(Ca) channels by 1 mM internal Ba^{2+} was determined in normal Ringer solution with the addition of 10 nM external NTX in order to block the voltage-gated K^+ channels (Fig. 12, *C* and *D*; see Fig. 15 for NTX block). The addition of 1 mM Ba^{2+} to the pipette solution resulted in voltage-dependent block with steepness almost identical to that seen with external Ba^{2+} (Fig. 12 *B*), but with opposite voltage dependence ($\delta = 0.26 \pm 0.05$;
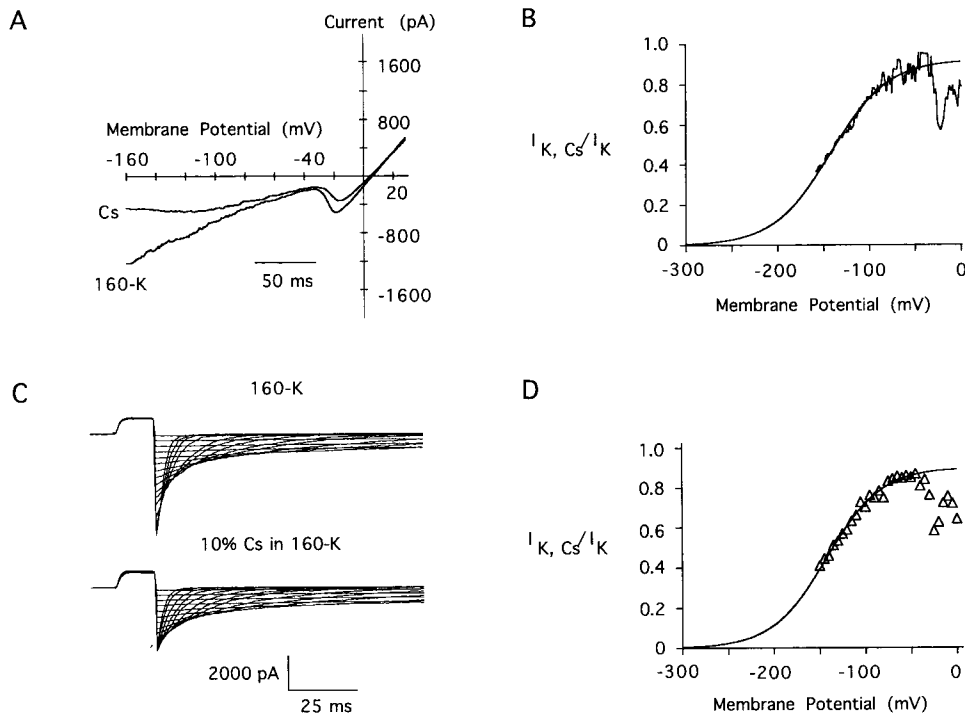
FIGURE 11. Cs⁺ block of K(Ca) and K(V) channels. K(Ca) channels were activated with whole-cell dialysis using pipette solutions containing 1 μM free Ca²⁺. (A) Ramp currents were recorded every 5 s. The bath solution was changed from K⁺ Ringer to a solution containing 90% K⁺ and 10% (16 mM) Cs⁺. (B) The ramp current trace obtained in the presence of Cs⁺ was divided by the trace obtained in the absence of Cs⁺ and plotted against the membrane potential. The smooth curve represents a fit (by eye) to the Boltzmann equation:

$$I_{K(Ca)Cs}/I_{K(Ca)} = 1/\{1 + \exp[(E_h - E)/k]\}$$

where E_h is the voltage at which half the channels are blocked and k is the steepness of block (millivolts per e-fold change). The parameters for the fits were $E_h = -135$ mV and $k = 32$ mV. (C) K(V) channels were activated with 15-ms depolarizing pulses to 40 mV every 10 s and then repolarized from −140 to 0 mV. The holding potential was −80 mV. The cell was bathed in K⁺ Ringer (top) and in K⁺ Ringer containing 16 mM Cs⁺ (bottom). The pipette solution in this experiment was KF. (D) The amplitude of the peak tail current in the presence of Cs⁺ divided by the peak tail current obtained without Cs⁺ gives the relative current at each potential. The Boltzmann fit shown by the smooth curve yielded parameters identical to those in B.

$k = -17 \pm 1$ mV; $n = 3$). These data indicate the existence of at least two Ba²⁺-binding sites within the K(Ca) pore.

In further experiments testing for effects of polyvalent cations, we found that externally applied La³⁺ and Co²⁺ blocked K(Ca) channels with half-block occurring at 0.17 and 20 mM, respectively. Ni²⁺ had no effect when applied externally at 5 mM. These same cations block K(V) channels almost completely at these concentrations (DeCoursey, Chandy, Gupta, and Cahalan, 1985, 1987a; data not shown).

Other blockers. External TEA is known to block voltage-gated K⁺ channels in HPB T lymphocytes ($K_d \approx 10$ mM; DeCoursey, Chandy, Gupta, and Cahalan, 1984; Grissmer and Cahalan, 1989a), and also blocks K(Ca) channels in Jurkat cells ($K_d \approx 2$ mM; Grissmer et al., 1992b). To compare the potency of TEA in blocking K(V)
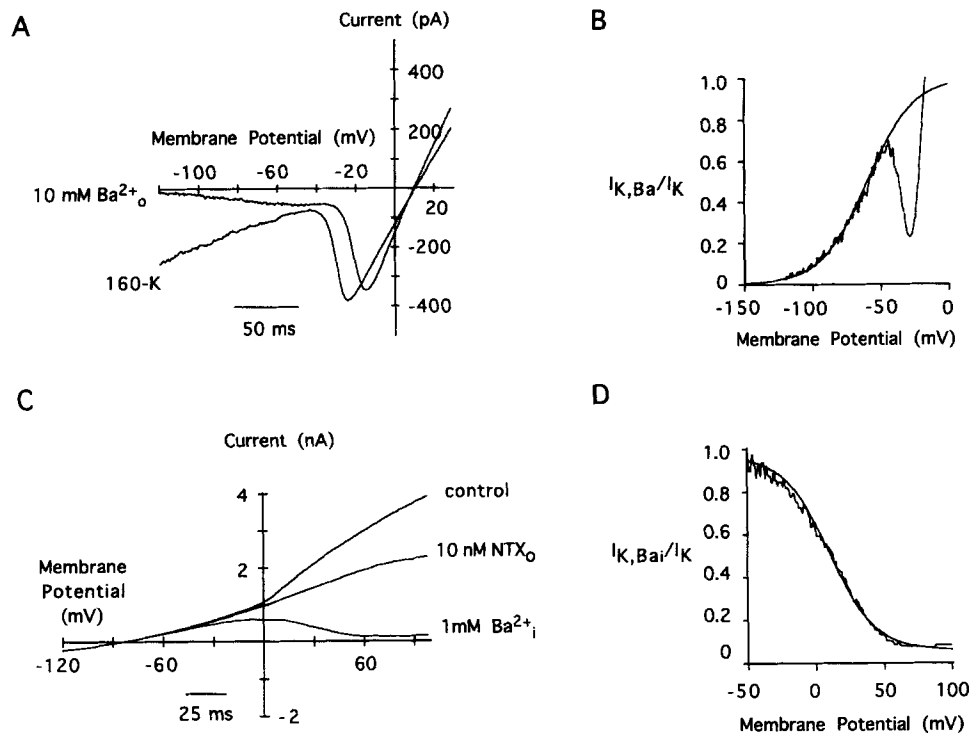
FIGURE 12.   External and internal Ba²⁺ block of K(Ca) channels in HPB T lymphocytes. K(Ca) channels were activated by whole-cell dialysis with pipette solutions containing 1 μM free Ca²⁺. (*A*) Ramp currents were elicited every 5 s. The bath solution was changed from K⁺ Ringer to K⁺ Ringer containing 10 mM Ba²⁺. (*B*) The ramp current trace obtained in the presence of external Ba²⁺ was divided by the trace obtained in the absence of Ba²⁺ and plotted against the membrane potential. The smooth curve represents a fit to a Boltzmann equation, as described in the legend to Fig. 11 *B*. The parameters for the fit were $E_h = -60$ mV and $k = 17$ mV. (*C*) Ramp currents were elicited every 10 s. After the bath solution was changed from normal Ringer solution (control) to normal Ringer + 10 nM NTX, the pipette solution was changed to one containing 1 mM Ba²⁺. (*D*) The ramp current trace obtained in the presence of internal Ba²⁺ was divided by the trace obtained in the absence of Ba²⁺ and plotted against the membrane potential. The smooth curve represents a fit to a Boltzmann equation as described in the legend to Fig. 11 *B*. The parameters for the fit were $E_h = 10$ mV and $k = -16.5$ mV.

and/or K(Ca) channels in activated HPB T lymphocytes, we performed parallel experiments on the same batch of cells using either KF as internal pipette solution ($[Ca^{2+}]_i < 10$ nM) to examine K(V) channels, or K-aspartate solutions buffered to 1 μM Ca²⁺ to examine both K(V) and K(Ca) channels. Fig. 13 *A* shows current through

K(V) channels in the absence and presence of different concentrations of TEA, confirming that 10 mM TEA blocks ~50% of the channels. K(Ca) channels in human T cells are more resistant to block by TEA, as can be seen from Fig. 13 B. The slope of the ramp current at negative potentials, a measure of K(Ca) channel activation,
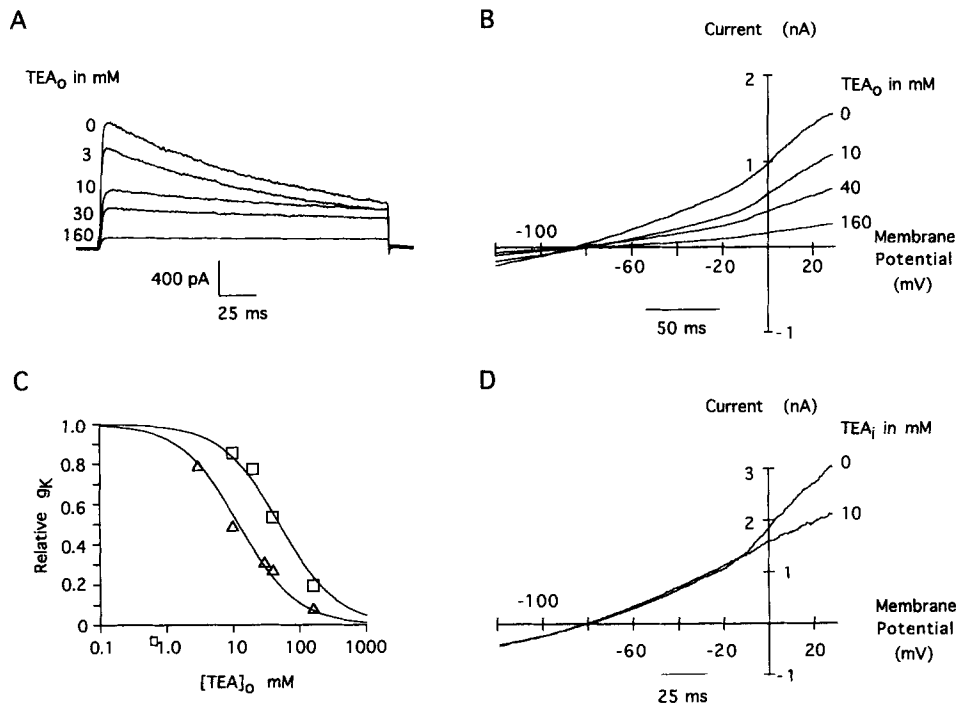

FIGURE 13. TEA$^+$ block of K(V) and K(Ca) channels in HPB T lymphocytes. (A) K(V) channels were activated with 200-ms depolarizing pulses to 40 mV every 30 s in the absence and presence of externally applied 3, 10, 30, and 160 mM TEA$^+$. KF pipette solution. (B) K(Ca) channels were activated with whole-cell dialysis with pipette solutions containing 1 μM free Ca^{2+}. Ramp currents were elicited every 10 s in the absence and presence of 10, 40, and 160 mM TEA$^+$. (C) Dose–response relationship for the block of K(V) channels (△) and K(Ca) channels (□). The lines through the points were fitted by eye to a modified Hill equation of the form:

$$I_{K(V,Ca)} = 1/[1 + (K_d/[TEA])]$$

with K_d's for K(V) and K(Ca) channel block of 10 and 40 mM, respectively. (D) K(Ca) channels were activated with whole-cell dialysis with pipette solutions containing 1 μM free Ca^{2+}. Ramp currents were elicited every 10 s before and after changing the pipette solution from TEA-free to 10 mM TEA.

decreased by about half with 40 mM TEA. Dose–response curves for TEA to block K(V) and K(Ca) channels in HPB T lymphocytes are shown in Fig. 13 C.

Internally applied TEA selectively blocks the K(V) channels (Fig. 13 D). The slope of the ramp current at negative potentials is unaffected by changing the TEA-free

internal pipette solution to a solution containing 10 mM TEA, whereas the current through K(V) channels is almost completely blocked.

Several other channel blockers were tested for effects on the K(Ca) channels in activated HPB T lymphocytes. 4-Aminopyridine (4AP) and quinine are known to block K(V) channels with K_d values of 150 and 20 μM, respectively (DeCoursey et al., 1984), but were less effective on K(Ca) channels; no effect of 4AP was seen at 1 mM, and quinine produced half-block at 50 μM. Apamin is an extremely potent blocker of K(Ca) channels in Jurkat T cells (K_d < 1 nM), but had no effect on K(Ca) channels in normal human resting or activated T cells at 100 nM.

Peptide toxins. In Jurkat T cells, the majority of K(Ca) channels is sensitive to block by apamin (K_d < 1 nM), a component of bee venom (Grissmer et al., 1992b). In HPB T lymphocytes, however, apamin up to 100 nM did not reduce the current through K(Ca) channels (data not shown). CTX, a purified scorpion toxin, was first described as a high affinity blocker of large conductance K(Ca) channels in a variety of cells, including skeletal muscle (Miller et al., 1985). CTX has also been found to be a potent blocker of K(V) channels in human T lymphocytes (Price, Lee, and Deutsch, 1989; Sands, Lewis, and Cahalan, 1989). In addition, a minor component of K(Ca) channels in Jurkat T cells was sensitive to block by CTX (Grissmer et al., 1992b). As shown in Fig. 14, application of different CTX concentrations blocked K(V) and K(Ca) channels in normal human T cells with identical potency (K_d of 3.5 nM; Fig. 14 C).

NTX, another purified scorpion toxin that shares some structural similarities with CTX (Strong, 1990), has also been shown to block K(V) channels in HPB T lymphocytes (Sands et al., 1989; Slaughter, Shevell, Felix, Lin, Sigal, and Kaczo-rowski, 1991). Fig. 15 A confirms that NTX blocks K(V) channels. Surprisingly, K(Ca) channels are resistant to block by NTX (Fig. 15 B). The dose–response curves for NTX to block K(V) and K(Ca) channels are about three orders of magnitude different (Fig. 15 C). These results lead to the conclusion that structural features of the external mouths of the two channel types are similar but not identical, since NTX can distinguish between K(V) and K(Ca) channels.

DISCUSSION

In this study, we have described the levels of functional expression, calcium dependence, ion selectivity and conductance, and pharmacological sensitivity of K(Ca) channels in human T lymphocytes. Our experiments have characterized a voltage-independent K⁺ channel that is highly sensitive to elevated $[Ca^{2+}]_i$. The channels opened rapidly and remained stable during whole-cell dialysis with pipette solutions containing elevated $[Ca^{2+}]_i$. In excised patches, we identified single K(Ca) channels that correspond to the whole-cell $g_{K(Ca)}$. The open channel rectifies weakly in symmetrical K⁺ with a conductance of 11–35 pS. Several aspects of ion permeation and block are similar in the K(Ca) channels and the voltage-gated type *n* K(V) channels that are found together in these cells, but some significant differences, in addition to the mode of gating, distinguish these channels. The similarity of CTX dose–response curves for K(V) and K(Ca) channels demonstrates that CTX cannot be used as a selective blocker of either channel.

Comparison of Lymphocyte K^+ Channels

Patch-clamp experiments on T lymphocytes have revealed several distinct types of ion channels, including K(V) channels, K(Ca) channels, osmotically regulated Cl^- channels, and mitogen-regulated Ca^{2+} channels (reviewed in Cahalan and Lewis, 1990; Cahalan, Chandy, and Grissmer, 1992; Chandy, Gutman, and Grissmer, 1993). Four types of K^+ channel in T cells have now been characterized biophysically in
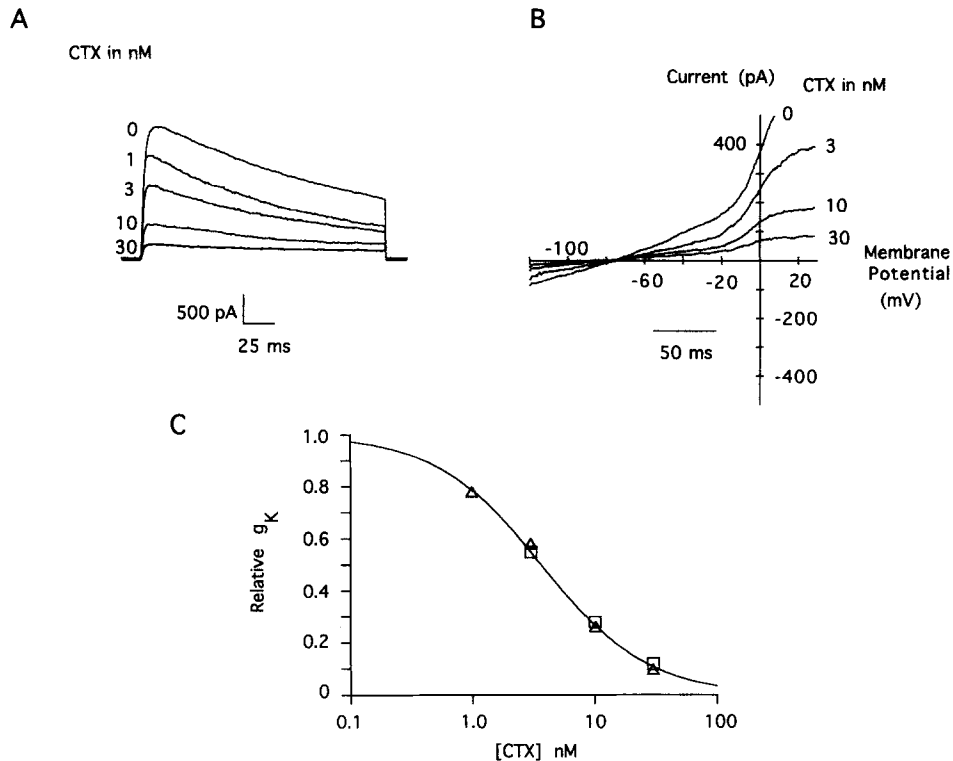

FIGURE 14. CTX block of K(V) and K(Ca) in HPB T lymphocytes. (*A*) K(V) channels were activated as in Fig. 13 *A* in the absence and presence of 1, 3, 10, and 30 nM CTX. (*B*) K(Ca) channels were activated as in Fig. 13 *B* in the absence and presence of 3, 10, and 30 nM CTX. (*C*) Dose–response relationship for the block of K(V) channels (△) and K(Ca) channels (□). The lines through the points were fitted by eye to a modified Hill equation as described in the legend of Fig. 13, with identical K_d's for K(V) and K(Ca) channel block of 3.5 nM.

some detail; in addition, there is evidence for other K^+ channels that occur in selected subsets or less abundantly (Lewis and Cahalan, 1988; Lee, Levy, and Deutsch, 1992). Types *n* and *l* K(V) channels differ in voltage dependence, inactivation, single-channel conductances, pharmacological properties, and distribution in T cell subsets (reviewed in Cahalan et al., 1992). These two K(V) channels have been cloned, sequenced, and expressed in oocytes and exogenous mammalian cells (Grissmer, Dethlefs, Wasmuth, Goldin, Gutman, Cahalan, and Chandy, 1990; Griss-

mer, Ghanshani, Dethlefs, McPherson, Wasmuth, Gutman, Cahalan, and Chandy, 1992a). In contrast, nothing is known about the structure of the lymphocyte K(Ca) channels at the molecular level.

The two types of K(Ca) channels found in lymphocytes include an apamin-sensitive, low-conductance (5 pS), voltage-independent channel that is found predominantly in Jurkat T cells, along with the CTX-sensitive K(Ca) channel described here. The apamin-sensitive channel in Jurkat cells may correspond to low conduc-
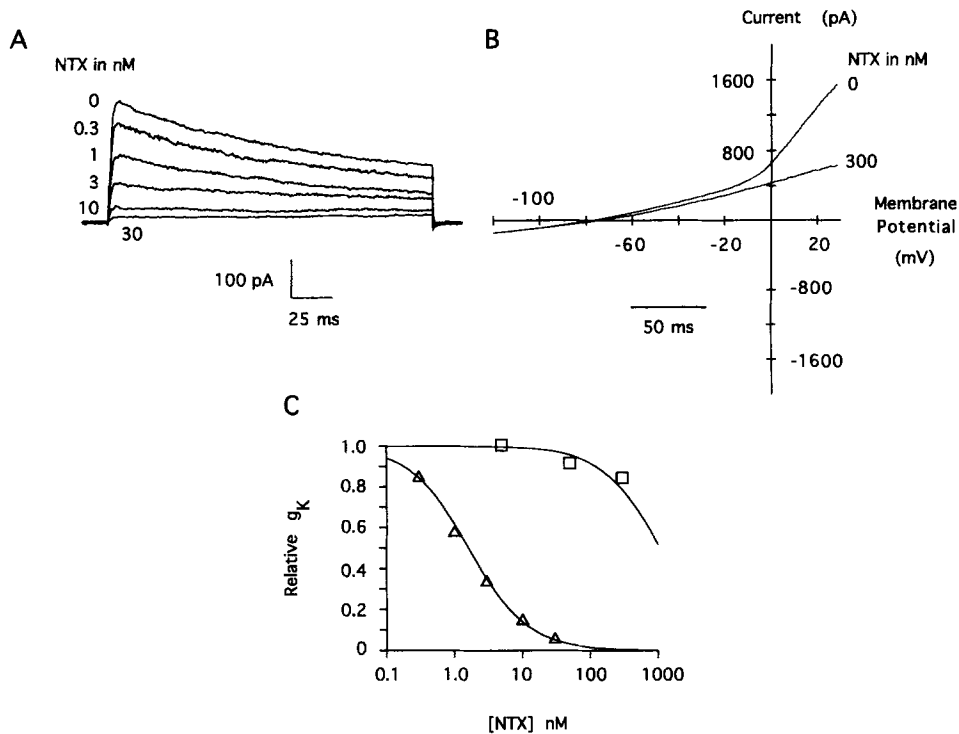

FIGURE 15. NTX block of K(V) and K(Ca) in HPB T lymphocytes. (*A*) K(V) channels were activated as in Fig. 14 *A* in the absence and presence of 0.3, 1, 3, and 10 nM NTX. (*B*) K(Ca) channels were activated as in Fig. 13 *B* in the absence and presence of 300 nM NTX. (*C*) Dose–response relationship for the block of K(V) channels (△) and K(Ca) channels (□). The lines through the points were fitted by eye to a modified Hill equation as described in the legend of Fig. 13, with K_d's for K(V) and K(Ca) channel block of 1.8 and 1,000 nM, respectively.

tance K(Ca) channels in single-channel patch experiments on human B lymphocytes and rat thymocytes (Mahaut-Smith and Schlichter, 1989; Mahaut-Smith and Mason, 1991). Our experiments indicate that the main type of K(Ca) channel seen in normal human T cells is a CTX-sensitive, voltage-independent K(Ca) channel with an inwardly rectifying single-channel conductance of 11–35 pS. This channel may correspond to the inwardly rectifying 25-pS channel seen in human B lymphocytes (Mahaut-Smith and Schlichter, 1989).

Both apamin- and CTX-sensitive K(Ca) channels exhibit little or no dependence on voltage, while sharing a similar dependence on $[Ca^{2+}]_i$, with a threshold for activation near 200 nM (Grissmer et al., 1992b; Fig. 5). The steepness of the $[Ca^{2+}]_i$ dependence suggests a cooperative mechanism of channel activation with several Ca^{2+}-binding sites. The CTX-sensitive K(Ca) channels exhibited the same $[Ca^{2+}]_i$ sensitivity in both whole-cell measurements using fura-2 to measure $[Ca^{2+}]_i$ and excised inside-out patch recordings with varying $[Ca^{2+}]$-EGTA-buffered solutions applied directly to the cytoplasmic membrane surface (Figs. 5 and 6). The calcium sensitivity can be accounted for by increases in P_o up to a maximum value of ~ 0.4 at saturating $[Ca^{2+}]_i$.

The type n K(V) channel and the CTX-sensitive K(Ca) channel share several properties associated structurally with the S5–S6 region of the Kv1.3 gene encoding the pore region of the type n channel. The biophysical and pharmacological similarities include single-channel conductance values of 11–35 pS with weak inward rectification in symmetrical K^+ (Cahalan et al., 1985; cf. Fig. 8), the sequence of ion selectivity (Fig. 10, Table I), voltage-dependent block by Cs^+ and Ba^{2+} (Figs. 11 and 12), and identical sensitivity to block by CTX (Fig. 14). The voltage dependence of block by external Ba^{2+} and Cs^+ suggests a common site at an "electrical distance" three-quarters of the way across the membrane from the outside. Interestingly, Ba^{2+} block from the inside is also strongly voltage dependent. A Ba^{2+} ion may be able to hop between two sites within the membrane across a low central barrier in order to pass nearly three-quarters across the membrane field from either side. Alternatively, there may be multiple Ba^{2+} ions, each traversing a smaller distance within the channel to account for the steep voltage dependence. Thus, K(Ca) channels may have at least two ion-binding sites within the electric field of the pore.

The biophysical similarities of K(Ca) and K(V) channels suggest underlying structural similarities in the region of the molecule that lines the pore. However, the channels differ in some aspects also associated with regions of the molecule near the pore. The selectivity of the K(Ca) channel for K^+ ions over Rb^+, NH_4^+, or Cs^+ is lower than in the K(V) channel (Table I). Block of K(V) channels by external TEA with a K_d of 10 mM is associated with His^{401}, which guards the "P region" within S5–S6 that is believed to form part of the open channel across the membrane (Busch, Hurst, North, Adelman, and Kavanaugh, 1991). The sensitivity of the K(Ca) channel to TEA is somewhat lower ($K_d = 40$ mM) than that of the K(V) channel (Fig. 13 C). Block by internal TEA in Shaker is associated with a conserved threonine, separated by only eight amino acids from the site of external TEA block (Yellen, Jurman, Abramson, and MacKinnon, 1991). The K(Ca) channel appears to be much less sensitive to internal TEA than is the K(V) channel (Fig. 13 D), implying a different structure at the inner mouth of the pore. Several residues within the S5–S6 region of Shaker and Kv1.3 have been associated with block by external peptide toxins such as CTX (MacKinnon and Miller, 1989; Goldstein and Miller, 1992). These residues may line an external vestibule approaching a selectivity filter region of the pore. In the corresponding region of the K(Ca) channel, Cs^+ and CTX may compete for binding (Fig. 10 D), as does TEA in the large conductance maxi-K(Ca) channel and in the lymphocyte type n K(V) channel (Miller, 1988; Chandy et al., 1993). The dose–response curves for CTX block of K(V) and K(Ca) channels were found to be identical, with a K_d of 3.5 nM (Fig. 14). Yet the two channels can be distinguished by

a similar peptide toxin, NTX, which blocks the K(V) channel with ~1,000-fold higher affinity (Fig. 15). Site-directed mutagenesis studies within the S5–S6 region of *Shaker*-related genes have demonstrated that conservative substitutions of amino acids can profoundly affect channel functions, including ion selectivity and block. We conclude that the K(Ca) channel is likely to have a closely similar, but not identical, sequence of amino acids that confers the properties of ion selectivity and block upon the Kv1.3 channel.

Comparison with K(Ca) Channels in Other Cells

The biophysical and pharmacological properties of K(Ca) channels provide a basis for comparison to K⁺ channels in other cell types. K(Ca) channels may be classified as voltage- and Ca^{2+}-dependent maxi-K⁺ (BK) channels with single-channel conductances >100 pS, or as SK channels that are voltage independent and have conductances <50 pS (reviewed by Latorre, Oberhauser, Labarca, and Alvarez, 1989). Within the latter category, apamin-sensitive K(Ca) channels have been described most frequently. Although found quite abundantly in Jurkat human leukemic T cells, the apamin-sensitive channels appear to be lacking in normal human resting and activated T cells. CTX was originally described as a blocker of maxi-K⁺ channels from skeletal muscle (reviewed by Latorre et al., 1989), but also blocks the type *n* K(V) channels in T cells (Sands et al., 1989), as well as the K(Ca) channels described here (Fig. 14).

The K(Ca) channels described here resemble those found in red blood cells, the cell type in which K(Ca) channels were first discovered through tracer flux measurements (Gárdos, 1958; reviewed by Schwarz and Passow, 1983). Subsequent patch-clamp experiments identified a $[Ca^{2+}]_i$-activated and voltage-independent K⁺ channel that underlies this efflux. The red cell K(Ca) channel's conductance is similar to that described here in T lymphocytes (Grygorczyk, Schwarz, and Passow, 1984; Leinders, van Kleef, and Vijverberg, 1992). The channel rectifies inwardly in symmetrical K⁺ (Grygorczyk et al., 1984) and is blocked by CTX in the nanomolar range (Wolff, Cecchi, Spalvins, and Canessa, 1988). One apparent difference is that the red cell K(Ca) channel is activated at higher $[Ca^{2+}]_i$ levels than reported here for K(Ca) channels in T cells (Grygorczyk et al., 1984; Leinders et al., 1992).

Similar K(Ca) channels have also been described in HeLa cells (Sauvé et al., 1986), macrophages (Gallin, 1989), and transformed fibroblasts (Huang and Rane, 1993). HeLa cells are a well-known permanent cell line derived from a cervical carcinoma. Voltage-independent K(Ca) channels in these cells exhibit weak inward rectification with a limiting conductance of 50 pS in symmetrical 200 mM [K⁺] (Sauvé et al., 1986). The $[Ca^{2+}]_i$ dependence of this channel corresponds closely with that reported here for K(Ca) channels in T lymphocytes; channel activation occurs when $[Ca^{2+}]_i$ rises above 100 nM and is complete at ~1 µM. *Ras*-transformed fibroblasts have a similar channel that is blocked by CTX, but appears to be less steeply dependent upon $[Ca^{2+}]_i$ (Huang and Rane, 1993).

Changes in Channel Expression That Precede Cell Division

Previous studies on resting and activated lymphocytes have found that the number of K(V) channels per cell increases after mitogenic activation. In human T cells, the number of type *n* K(V) channels per cell increases, but the density of these channels

probably remains about the same; in our experiments using T cells activated for 3–6 d, we found a 3.4-fold increase in $g_{K(V)}$ compared with resting cells, an increase that paralleled the increase in surface area of cells selected for patch clamping in the population. Deutsch and colleagues found an increase in $g_{K(V)}$ of 1.7-fold for 1- and 2-d PHA-activated T cells after mitogenic activation (Deutsch, Krause, and Lee, 1986). In mouse T cells, a relatively larger increase in the number of K(V) channels after mitogenic activation represents an increase in the density of K(V) channels; the number of these channels in resting murine T cells is lower than in resting human T cells (DeCoursey, Chandy, Gupta, and Cahalan, 1987b).

Here, we have shown that the number of conducting K(Ca) channels in human T lymphocytes increases by > 20-fold after mitogenic activation (Fig. 2). Taking into account the maximum P_o of < 0.5 from single-channel measurements (Figs. 6–8), the number of channels is likely to be > 1,000 per cell in T cell blasts and ~ 40 in resting T cells. Considering the membrane surface areas estimated from capacitance measurements, a reasonable estimate for K(Ca) channel densities is $0.2/\mu m^2$ in resting T cells and $2/\mu m^2$ in T cell blasts. In preliminary experiments, we have seen increases in K(Ca) channels of similar magnitude in activated mouse T cells (Grissmer, S., A. N. Nguyen, and M. D. Cahalan, unpublished observations). Human and murine B lymphocytes also undergo changes in the expression of both K(V) and K(Ca) channels that parallel mitogenic activation (Sutro, Vayuvegula, Gupta, and Cahalan, 1989; Partiseti et al., 1992). Increased expression of K(Ca) channels is also associated with cell proliferation in ras-transformed fibroblasts (Huang and Ray, 1993).

Physiological Role of K(Ca) Channels in Lymphocytes

The resting potential of T cells is maintained primarily by K(V) channels in the quiescent state of the cell when $[Ca^{2+}]_i$ is low (Cahalan et al., 1985; Grinstein and Smith, 1990; Leonard, Garcia, Slaughter, and Reuben, 1992). The existence of K(Ca) channels and their possible role in mediating membrane hyperpolarization during the Ca^{2+} signal elicited by T cell receptor stimulation has been postulated for some time (Tsien et al., 1982). We have demonstrated that the K(Ca) channels described here exhibit the sensitivity needed to become active during a rise in $[Ca^{2+}]_i$ above a resting value of ~ 100 nM. Do K(Ca) channels contribute to $[Ca^{2+}]_i$ signaling in T cells? As $[Ca^{2+}]_i$ begins to rise, due initially to release of Ca^{2+} from internal stores and later to Ca^{2+} entry through voltage-independent Ca^{2+} channels, K(Ca) channels become activated and the resulting hyperpolarization may in turn contribute to enhanced $[Ca^{2+}]_i$ entry by increasing the driving force (Lewis and Cahalan, 1989, 1990). This positive feedback mechanism could promote the upstroke of the oscillatory $[Ca^{2+}]_i$ signal in T cells. In Jurkat cells, we have previously demonstrated that $[Ca^{2+}]_i$ oscillations are disrupted by simultaneous blockade of both K(V) and K(Ca) channels, but are less affected by selective block of just one channel type (Grissmer et al., 1992b). As we have shown here, the predominant K(Ca) channel in resting human T cells is the CTX-sensitive K(Ca) channel, with only 20 channels per cell being able to conduct when $[Ca^{2+}]_i$ is elevated. In these resting cells, blockade of the K(V) channels with NTX, which we have shown to be selective for K(V) channels (Fig. 15), inhibits both a component of the $[Ca^{2+}]_i$ signal and mitogen-stimulated T cell proliferation (Slaughter et al., 1991). Therefore, in resting T cells with low K(Ca)

expression, it appears that K(V) channels may be more significant than K(Ca) channels in maintaining the electrical driving force to sustain Ca^{2+} entry. On the other hand, the increased number of K(Ca) channels in T cell blasts correlates with their enhanced ability to generate sustained and oscillatory $[Ca^{2+}]_i$ signals upon T cell receptor stimulation (Hess, Oortgiesen, and Cahalan, 1993). Thus, we suggest that K(Ca) channels may play an increasingly significant role in $[Ca^{2+}]_i$ signaling during the reactivation of T cells. Selective blockers may help to address the relative contributions of K(Ca) and K(V) channels to the membrane potential and indirectly to $[Ca^{2+}]_i$ signaling during T cell activation.

REFERENCES

Almers, W., and E. Neher. 1985. The Ca signal from fura-2 loaded mast cells depends strongly on the method of dye-loading. *FEBS Letters.* 192:13–18.

Bregestovski, P., A. Redkozubov, and A. Alexeev. 1986. Elevation of intracellular calcium reduces voltage-dependent potassium conductance in human T cells. *Nature.* 319:776–778.

Busch, A. E., R. S. Hurst, R. A. North, J. P. Adelman, and M. P. Kavanaugh. 1991. Current inactivation involves a histidine residue in the pore of the rat lymphocyte potassium channel RGK5. *Biochemical and Biophysical Research Communications.* 179:1384–1390.

Cahalan, M. D., K. G. Chandy, T. E. DeCoursey, and S. Gupta. 1985. A voltage-gated K⁺ channel in human T lymphocytes. *Journal of Physiology.* 358:197–237.

Cahalan, M. D., K. G. Chandy, and S. Grissmer. 1992. Potassium channels in development, activation, and disease in T lymphocytes. *Current Topics in Membranes.* 39:357–394.

Cahalan, M. D., and R. S. Lewis. 1990. Functional roles of ion channels in lymphocytes. *Seminars in Immunology.* 2:107–117.

Chandy, K. G., G. A. Gutman, and S. Grissmer. 1993. Physiological role, molecular structure, and evolutionary relationships of voltage-gated potassium channels in T lymphocytes. *Seminars in the Neurosciences.* 5:125–134.

Crabtree, G. R. 1989. Contingent genetic regulatory events in T lymphocyte activation. *Science.* 243:355–361.

DeCoursey, T. E., K. G. Chandy, S. Gupta, and M. D. Cahalan. 1984. Voltage-gated K channels in human T lymphocytes: a role in mitogenesis? *Nature.* 307:465–468.

DeCoursey, T. E., K. G. Chandy, S. Gupta, and M. D. Cahalan. 1985. Voltage-dependent ion channels in T lymphocytes. *Journal of Neuroimmunology.* 10:71–85.

DeCoursey, T. E., K. G. Chandy, S. Gupta, and M. D. Cahalan. 1987a. Two types of potassium channels in murine T lymphocytes. *Journal of General Physiology.* 89:379–404.

DeCoursey, T. E., K. G. Chandy, S. Gupta, and M. D. Cahalan. 1987b. Mitogen induction of ion channels in murine T lymphocytes. *Journal of General Physiology.* 89:405–420.

Deutsch, C., D. Krause, and S. C. Lee. 1986. Voltage-gated potassium conductance in human T lymphocytes stimulated with phorbol ester. *Journal of Physiology.* 372:405–423.

Felber, S. B., and M. D. Brand. 1983. Early plasma-membrane potential changes during stimulation of lymphocytes by concanavalin A. *Biochemical Journal.* 210:885–891.

Gallin, E. K. 1989. Evidence for a Ca-activated inwardly rectifying K channel in human macrophages. *American Journal of Physiology*. 257:C77–C85.

Gárdos, G. 1958. The function of calcium v in the potassium permeability of human erythrocytes. *Biochimica et Biophysica Acta*. 30:653–654.

Gelfand, E. W., R. K. Cheung, and S. Grinstein. 1984. Role of membrane potential in the regulation of lectin-induced calcium uptake. *Journal of Cellular Physiology*. 121:533–539.

Goldstein, S. A. N., and C. Miller. 1992. A point mutation in a *Shaker* K⁺ channel changes its charybdotoxin binding site from low to high affinity. *Biophysical Journal*. 62:5–7.

Grinstein, S., and S. J. Dixon. 1989. Ion transport and membrane potential in lymphocytes: changes during activation. *Physiological Reviews*. 69:417–482.

Grinstein, S., and J. D. Smith. 1990. Calcium-independent cell volume regulation in human lymphocytes. *Journal of General Physiology*. 95:97–120.

Grissmer, S., and M. D. Cahalan. 1989a. TEA prevents inactivation while blocking open K⁺ channels in human T lymphocytes. *Biophysical Journal*. 55:203–206.

Grissmer, S., and M. D. Cahalan. 1989b. Divalent ion trapping inside potassium channels of human T lymphocytes. *Journal of General Physiology*. 93:609–630.

Grissmer, S., and M. D. Cahalan. 1991. Ca²⁺-activated K⁺ channels in resting and activated human peripheral T lymphocytes. *Biophysical Journal*. 59:213a. (Abstr.)

Grissmer, S., B. Dethlefs, J. Wasmuth, A. L. Goldin, G. A. Gutman, M. D. Cahalan, and K. G. Chandy. 1990. Expression and chromosomal localization of a lymphocyte K⁺ channel gene. *Proceedings of the National Academy of Sciences, USA*. 87:9411–9415.

Grissmer, S., S. Ghanshani, B. Dethlefs, J. McPherson, J. Wasmuth, G. A. Gutman, M. D. Cahalan, and K. G. Chandy. 1992a. The *Shaw*-related potassium-channel gene, Kv3.1, on human chromosome 11, encodes the type *l* K⁺ channel in T cells. *Journal of Biological Chemistry*. 267:20971–20979.

Grissmer, S., R. S. Lewis, and M. D. Cahalan. 1992b. Ca²⁺-activated K⁺ channels in human leukemic T cells. *Journal of General Physiology*. 99:63–84.

Grissmer, S., A. N. Nguyen, and M. D. Cahalan. 1992c. Characterization of Ca²⁺-activated K⁺ channels in resting and activated human peripheral T lymphocytes. *Biophysical Journal*. 61:A14. (Abstr.)

Grygorczyk, R., W. Schwarz, and H. Passow. 1984. Ca²⁺-activated K⁺ channels in human red cells. Comparison of single-channel currents with ion fluxes. *Biophysical Journal*. 45:693–698.

Hamill, O. P., A. Marty, E. Neher, B. Sakmann, and F. J. Sigworth. 1981. Improved patch-clamp techniques for high-resolution current recording from cells and cell-free membrane patches. *Pflügers Archiv*. 391:85–100.

Hess, S. D., M. Oortgiesen, and M. D. Cahalan. 1993. Calcium oscillations in human T and NK cells depend upon membrane potential and calcium influx. *Journal of Immunology*. 150:2620–2633.

Hill, A. V. 1910. The possible effects of the aggregation of the molecules of haemoglobin on its dissociation curves. *Journal of Physiology*. 40:iv–vii.

Huang, Y., and S. G. Rane. 1993. Single channel study of a Ca²⁺-activated K current associated with *ras*-induced cell transformation. *Journal of Physiology*. 461:601–618.

Imboden, J. B., and J. D. Stobo. 1985. Transmembrane signalling by the T cell antigen receptor. *Journal of Experimental Medicine*. 161:446–456.

June, C. H., J. A. Ledbetter, P. S. Rabinovitch, P. J. Martin, P. G. Beatty, and J. A. Hansen. 1986. Distinct patterns of transmembrane calcium flux and intracellular calcium mobilization after differentiation antigen cluster 2 (E rosette receptor) or 3 (T3) stimulation of human lymphocytes. *Journal of Clinical Investigation*. 77:1224–1232.

Kuno, M., J. Goronzy, C. M. Weyand, and P. Gardner. 1986. Single-channel and whole-cell recordings of mitogen-regulated inward currents in human cloned helper T lymphocytes. *Nature*. 323:269–273.

Latorre, R., A. Oberhauser, P. Labarca, and O. Alvarez. 1989. Varieties of calcium-activated potassium channels. *Annual Review of Physiology.* 51:385–399.

Lee, S. C., D. I. Levy, and C. Deutsch. 1992. Diverse K^+ channels in primary human T lymphocytes. *Journal of General Physiology.* 99:771–793.

Leinders, T., R. G. van Kleef, and H. P. Vijverberg. 1992. Single Ca^{2+}-activated K^+ channels in human erythrocytes: Ca^{2+} dependence of opening frequency but not of open lifetimes. *Biochimica et Biophysica Acta.* 1112:67–74.

Leonard, R., M. L. Garcia, R. Slaughter, and J. P. Reuben. 1992. Selective blockers of voltage-gated K^+ channels depolarize human T lymphocytes: mechanism of the antiproliferative effect of charybdotoxin. *Proceedings of the National Academy of Sciences, USA.* 89:10094–10098.

Lewis, R. S., and M. D. Cahalan. 1988. Subset-specific expression of potassium channels in developing murine T lymphocytes. *Science.* 239:771–775.

Lewis, R. S., and M. D. Cahalan. 1989. Mitogen-induced oscillations of cytosolic Ca^{2+} and transmembrane Ca^{2+} current in human leukemic T cells. *Cell Regulation.* 1:99–112.

Lewis, R. S., and M. D. Cahalan. 1990. Ion channels and signal transduction in lymphocytes. *Annual Review of Physiology.* 52:415–430.

Lewis, R. S., S. Grissmer, and M. D. Cahalan. 1991. Role of K^+ channels in regulating calcium signaling in leukemic T lymphocytes. *Biophysical Journal.* 59:13a. (Abstr.)

MacDougall, S., S. Grinstein, and E. W. Gelfand. 1988. Activation of Ca^{2+}-dependent K^+ channels in human B lymphocytes by anti-immunoglobulin. *Journal of Clinical Investigation.* 81:449–454.

MacKinnon, R., and C. Miller. 1989. Mutant potassium channels with altered binding of charybdotoxin, a pore-blocking peptide inhibitor. *Science.* 245:1382–1387.

Mahaut-Smith, M. P., and M. J. Mason. 1991. Ca^{2+}-activated K^+ channels in rat thymic lymphocytes: activation by concanavalin A. *Journal of Physiology.* 439:513–528.

Mahaut-Smith, M. P., and L. C. Schlichter. 1989. Ca^{2+}-activated K^+ channels in human B lymphocytes and rat thymocytes. *Journal of Physiology.* 415:69–83.

Miller, C., E. Moczydlowski, R. Latorre, and M. Phillips. 1985. Charybdotoxin, a protein inhibitor of Ca^{2+}-activated K^+ channels from mammalian skeletal muscle. *Nature.* 313:316–318.

Miller, C. 1988. Competition for block of a Ca^{2+}-activated K^+ channel by charybdotoxin and tetraethylammonium. *Neuron.* 1:1003–1006.

Negulescu, P. A., and T. E. Machen. 1991. Intracellular ion activities and membrane transport in parietal cells measured with fluorescent dyes. *Methods in Enzymology.* 192:38–81.

Nguyen, A. N., M. D. Cahalan, and S. Grissmer. 1992. Properties and abundance of Ca^{2+}-activated K^+ channels in human peripheral T lymphocytes. *Society for Neuroscience Abstracts.* 18:74. (Abstr.)

Oettgen, H. C., C. Terhorst, L. C. Cantley, and P. M. Rosoff. 1985. Stimulation of the T3-T cell receptor complex induces a membrane-potential-sensitive calcium influx. *Cell.* 40:583–590.

Partiseti, M., D. Choquet, A. Diu, and H. Korn. 1992. Differential regulation of voltage- and calcium-activated potassium channels in human B lymphocytes. *Journal of Immunology.* 148:3361–3368.

Portzehl, H., P. C. Caldwell, and J. C. Ruegg. 1964. The dependence of contraction and relaxation of muscle fibres from the crab *Maia squinado* on the internal concentration of free calcium ions. *Biochimica et Biophysica Acta.* 79:581–591.

Price, M., S. C. Lee, and C. Deutsch. 1989. Charybdotoxin inhibits proliferation and interleukin 2 production in human peripheral blood lymphocytes. *Proceedings of the National Academy of Sciences, USA.* 86:10171–10175.

Rink, T. J., and C. Deutsch. 1983. Calcium-activated potassium channels in lymphocytes. *Cell Calcium.* 4:463–473.

Sands, S. B., R. S. Lewis, and M. D. Cahalan. 1989. Charybdotoxin blocks voltage-gated K^+ channels in human and murine T lymphocytes. *Journal of General Physiology.* 93:1061–1074.

Sauvé, R., C. Simoneau, R. Monette, and G. Roy. 1986. Single-channel analysis of the potassium permeability in HeLa cancer cells: evidence for a calcium-activated potassium channel of small unitary conductance. *Journal of Membrane Biology.* 92:269–282.

Schwarz, W., and H. Passow. 1983. Ca^{2+}-activated K^+ channels in erythrocytes and excitable cells. *Annual Review of Physiology.* 45:359–374.

Slaughter, R. S., J. L. Shevell, J. P. Felix, C. S. Lin, N. H. Sigal, and G. J. Kaczorowski. 1991. Inhibition by toxins of charybdotoxin binding to the voltage-gated potassium channel of lymphocytes. Correlation with block of activation of human peripheral T-lymphocytes. *Biophysical Journal.* 59:213a. (Abstr.)

Strong, P. N. 1990. Potassium channel toxins. *Pharmacology & Therapeutics.* 46:137–162.

Sutro, J. B., B. S. Vayuvegula, S. Gupta, and M. D. Cahalan. 1989. Voltage-sensitive ion channels in human B lymphocytes. *Advances in Experimental Medicine and Biology.* 254:113–122.

Tatham, P. E. R., K. O'Flynn, and D. C. Linch. 1986. The relationship between mitogen-induced membrane potential change and intracellular free calcium in human T lymphocytes. *Biochimica et Biophysica Acta.* 856:202–211.

Tsien, R. Y., T. Pozzan, and T. J. Rink. 1982. T-cell mitogens cause early changes in cytoplasmic free Ca^{2+} and membrane potential in lymphocytes. *Nature.* 295:68–71.

Wilson, H. A., and T. M. Chused. 1985. Lymphocyte membrane potential and Ca^{2+}-sensitive potassium channels described by oxonol dye fluorescence measurements. *Journal of Cellular Physiology.* 125:72–81.

Wolff, D., X. Cecchi, A. Spalvins, and M. Canessa. 1988. Charybdotoxin blocks with high affinity the Ca-activated K^+ channel of Hb A and Hb S red cells: individual differences in the number of channels. *Journal of Membrane Biology.* 106:243–252.

Yellen, G., M. E. Jurman, T. Abramson, and R. MacKinnon. 1991. Mutations affecting internal TEA blockade identify the probable pore-forming region of a K^+ channel. *Science.* 251:939–942.